CONFIDENTIAL

230
Copy
RM L9I07

NACA

RESEARCH MEMORANDUM

INVESTIGATION OF THE NACA 4-(4)(06)-04 TWO-BLADE PROPELLER AT FORWARD MACH NUMBERS TO 0.925

By James B. Delano and Daniel E. Harrison

Langley Aeronautical Laboratory
Langley Air Force Base, Va.

CLASSIFICATION CHANGED TO UNCLASSIFIED

AUTHORITY: J.W. CROWLEY DATE: 8-13-54

CHANGE #2474 WHL

NATIONAL ADVISORY COMMITTEE FOR AERONAUTICS

WASHINGTON
October 28, 1949

CONFIDENTIAL

NATIONAL ADVISORY COMMITTEE FOR AERONAUTICS

RESEARCH MEMORANDUM

INVESTIGATION OF THE NACA 4-(4)(06)-04 TWO-BLADE PROPELLER AT FORWARD MACH NUMBERS TO 0.925

By James B. Delano and Daniel E. Harrison

SUMMARY

Investigations of the NACA 4-(4)(06)-04 two-blade propeller (design thickness ratio, 0.06 at 0.7-radius station) have been made in the Langley 8-foot high-speed tunnel for blade angles from 20° to 70° for forward Mach numbers up to 0.925.

In general, the effects of compressibility on maximum efficiency are similar to those reported earlier for the NACA 4-(5)(08)-03 propeller. The envelope efficiency for the NACA 4-(4)(06)-04 propeller is 10 percent higher than that for the NACA 4(5)(08)-03 propeller at a forward Mach number of 0.8.

INTRODUCTION

Results of the first two phases of a general investigation to study the effects of compressibility, design camber, blade sweep, thickness ratio, and dual rotation on propeller performance at transonic speeds were presented in references 1 and 2. The effects of blade sweep on propeller performance constitute the next phase of this general investigation.

In the course of the investigation to study the effect of blade sweep on propeller performance a thin (6-percent thickness ratio) straight blade was tested to provide a comparison of results for swept and unswept blades. It was believed that the results obtained for this thin propeller would be of immediate interest and consequently are presented herein. The investigation was made for a range of blade angle from 20° to 70° for a forward Mach number range from 0.175 to 0.925.

Force-test results and a limited analysis for only the unswept propeller are presented at this time to expedite publication of this information. Large-scale plots of the basic propeller characteristics (fig. 5) are available on request to the NACA.

SYMBOLS

b	blade width, feet
c_{l_d}	blade-section design lift coefficient
C_P	power coefficient $\left(P/\rho n^3 D^5\right)$
C_T	thrust coefficient $\left(T/\rho n^2 D^4\right)$
D	propeller diameter, feet
b/D	blade width ratio
h	maximum thickness of blade section, feet
h/b	blade thickness ratio
J	advance ratio $\left(V_o/nD\right)$
M	tunnel-datum (forward) Mach number (tunnel Mach number uncorrected for tunnel-wall constraint)
M_t	helical tip Mach number $\left(M\sqrt{1 + \frac{\pi^2}{J^2}}\right)$
n	propeller rotational speed, revolutions per second
P	power, foot-pounds per second
q	dynamic pressure, pounds per square foot $\left(\rho V^2/2\right)$
R	propeller-tip radius, feet
r	blade-section radius, feet
T	thrust, pounds

T_c thrust disk-loading coefficient $\left(T/2qD^2\right)$

V tunnel-datum velocity (tunnel velocity uncorrected for tunnel-wall constraint), feet per second

V_o equivalent free-air velocity (tunnel-datum velocity corrected for tunnel-wall constraint), feet per second

x blade-section station (r/R)

β section blade angle, degrees

$\beta_{0.7R}$ section blade angle at 0.7 tip radius, degrees

η efficiency $\left(\frac{C_T}{C_P} J\right)$

η_{max} maximum efficiency

ρ air density, slugs per cubic foot

APPARATUS, METHODS, AND TESTS

The apparatus and methods described in reference 1 were used in this investigation which was conducted in the Langley 8-foot high-speed tunnel. A sketch of the 800-horsepower dynamometer installed in the tunnel is shown as figure 1.

The NACA 4-(4)(06)-04 two-blade propeller used in this investigation is the unswept propeller of a family of propellers designed to study the effect of blade sweep on propeller characteristics at transonic speeds. It utilizes NACA 16-series airfoil sections and was designed as a two-blade propeller to produce minimum energy losses (profile drag assumed equal to zero) at a blade angle of 60° at the 0.7-radius station and at an advance ratio of 3.65. The gaps between the spinner and blades were sealed for all operating conditions. Blade-form curves are given in figure 2, and a photograph of the blades is shown in figure 3.

Thrust, torque, and rotational speed were measured throughout the complete operating range of the propeller. For each tunnel Mach number the propeller was run at a constant blade angle and the rotational speed was varied. The range of blade angle covered for each forward Mach number is given in the following table:

Forward Mach number, M	Blade angle at 0.7–radius station, $\beta_{0.7R}$ (deg)										
0.175	20	25	30								
.23	20	25	30	35		45					
.35			30	35	40		50		60		
.43				35	40	45		55		65	
.53					40	45	50	55	60		
.60						45	50	55		65	
.65						45	50	55	60	65	
.70							50	55		65	
.75							50	55	60	65	70
.80								55	60	65	70
.85									60	65	70
.90									60	65	
.925										65	

REDUCTION OF DATA

Propeller thrust.– Propeller thrust, as used herein, is defined as the shaft tension produced by the spinner–to–tip portion of the blades. The method used in determining thrust tares and in evaluating the propeller thrust is described in detail in reference 1.

Propeller torque.– Torque–tare corrections were found to be small and depended only on spinner rotational speed. The indicated torque reading was corrected for the spinner tare (a maximum of 1.2 foot–pounds at 6000 rpm).

Tunnel-wall correction.- The force-test data have been corrected for the effect of tunnel-wall constraint on velocity at the propeller test plane by using the method described in reference 1. These results are presented in figure 4 as the ratio of free-air velocity to the tunnel-datum velocity as a function of thrust disk-loading coefficient and tunnel-datum Mach number.

Accuracy of results.- Analysis of the accuracy of the separate measurements required to define fully the propeller characteristics has indicated that errors in the results presented herein are probably less than ±1 percent. Repeat runs have shown that the data can be reproduced to within ±1 percent.

RESULTS AND DISCUSSION

The basic propeller characteristics are presented in figure 5. For each value of tunnel-datum Mach number M the propeller thrust and power coefficients and efficiency are plotted against advance ratio. The variation of tip Mach number with advance ratio is also included. As used herein, the tunnel-datum Mach number M is not corrected for tunnel-wall constraint. The free-air Mach number, however, can be obtained by applying the tunnel-wall corrections, presented in figure 4, to the tunnel-datum Mach number. At the high Mach numbers the tunnel-wall correction is generally less than 1 percent but, in the exact use of the propeller characteristics presented in figure 5 wherever small changes in Mach number produce large changes in propeller characteristics, the tunnel-datum Mach number should be corrected to free-air Mach number.

Attention is called to the use of the blade angle $\beta_{0.7R}$ at the 0.7-radius station to designate the pitch setting of the blades for this investigation.

Effect of forward Mach number on maximum efficiency.- The variation of maximum efficiency with forward Mach number is presented in figure 6 for all the blade angles investigated. Results for a blade angle of 70° were obtained only for forward Mach numbers of 0.75, 0.80, and 0.85 because a crack developed in one of the blades and thereby prohibited further investigation of this propeller. In general, the results are similar to those presented in reference 1 for the NACA 4-(5)(08)-03 propeller.

The maximum delay in the onset of adverse compressibility effects was obtained for a blade angle of 70° $\left(\beta_{0.75R} \approx 68^{\circ}\right)$ in comparison to a blade angle $\left(\beta_{0.75R}\right)$ of 65° for the NACA 4-(5)(08)-03 propeller. This result occurs primarily because of the difference in design pitch.

Effect of advance ratio and forward Mach number on maximum efficiency.– The variation of maximum efficiency with advance ratio for the forward Mach numbers at which the propeller was investigated is shown in figure 7. In general, the results are similar to those presented in reference 1 for the NACA 4–(5)(08)–03 propeller except that the forward Mach number defining the transition from operation at high advance ratio to operation at low advance ratio for highest efficiencies is higher for the NACA 4–(4)(06)–04 propeller ($M = 0.85$). These results indicate that thinning the blade makes this transition occur at higher forward Mach numbers. Eventually, however, as the forward Mach number is increased the propeller will be operating as a supersonic type of propeller and the highest efficiencies will then be obtained at low values of advance ratio.

Comparison of envelope efficiency for NACA 4–(4)(06)–04 and 4–(5)(08)–03 propellers.– The envelope of the maximum–efficiency curves in figure 6 is presented in figure 8. A similar envelope curve for the NACA 4–(5)(08)–03 propeller from results of reference 1 is also presented in figure 8. At low forward Mach numbers there is little difference in envelope efficiency. At supercritical Mach numbers the rate of efficiency loss is less for the thin propeller, and at a forward Mach number of 0.80 the efficiency of the thin propeller is about 10 percent higher than for the NACA 4–(5)(08)–03 propeller. These differences in efficiency are caused by differences in thickness ratio and design pitch. The effect due to differences in design lift coefficient is believed to be secondary, as is shown by the comparison of results (reference 2) for the NACA 4–(3)(08)–03 and 4–(5)(08)–03 propellers.

CONCLUSIONS

Investigations of an NACA 4–(4)(06)–04 two–blade propeller in the Langley 8–foot high–speed tunnel for blade angles of 20° to 70° and through a forward Mach number range extending up to 0.925 and comparison of results with those for the NACA 4–(5)(08)–03 propeller (NACA RM L9G06a) indicate the following conclusions:

1. In general, the effects of compressibility on maximum efficiency are similar to those for the NACA 4–(5)(08)–03 propeller.

2. At a forward Mach number of 0.8 the envelope efficiency for the thin–blade propeller is 10 percent higher than that for the NACA

Page intentionally left blank

missing
8, 10, 12, 14

Page intentionally left blank

4-(5)(08)-03 propeller. This higher efficiency is attributed to the combination of reduced thickness ratio and a more favorable pitch distribution for the thinner propeller.

Langley Aeronautical Laboratory
National Advisory Committee for Aeronautics
Langley Air Force Base, Va.

REFERENCES

1. Delano, James B., and Carmel, Melvin M.: Investigation of the NACA 4-(5)(08)-03 Two-Blade Propeller at Forward Mach Numbers to 0.925. NACA RM L9G06a, 1949.

2. Delano, James B., and Morgan, Francis G., Jr.: Investigation of the NACA 4-(3)(08)-03 Two-Blade Propeller at Forward Mach Numbers to 0.925. NACA RM L9I06, 1949.

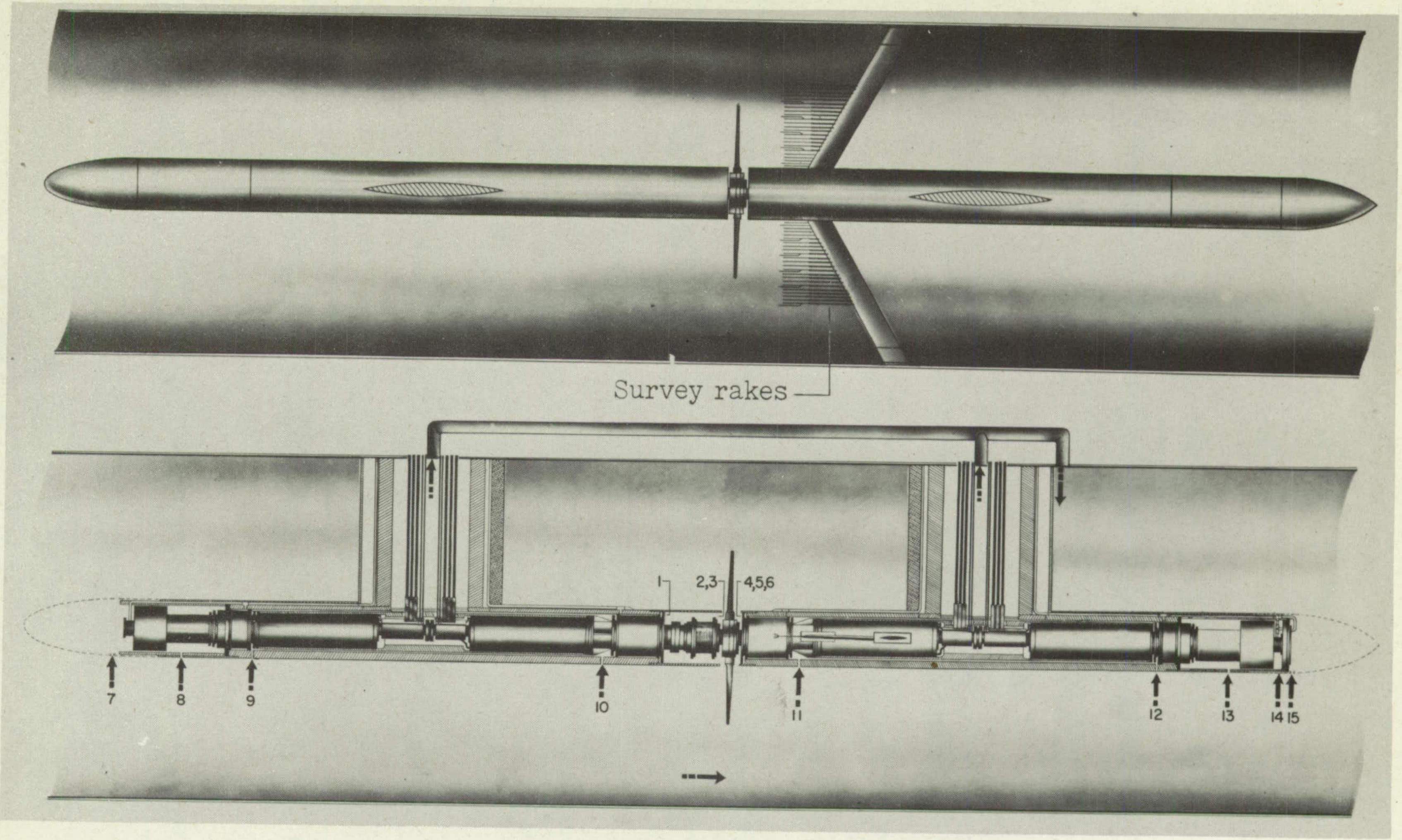

Figure 1.– Installation of propeller dynamometer in Langley 8–foot high–speed tunnel.

L-61063

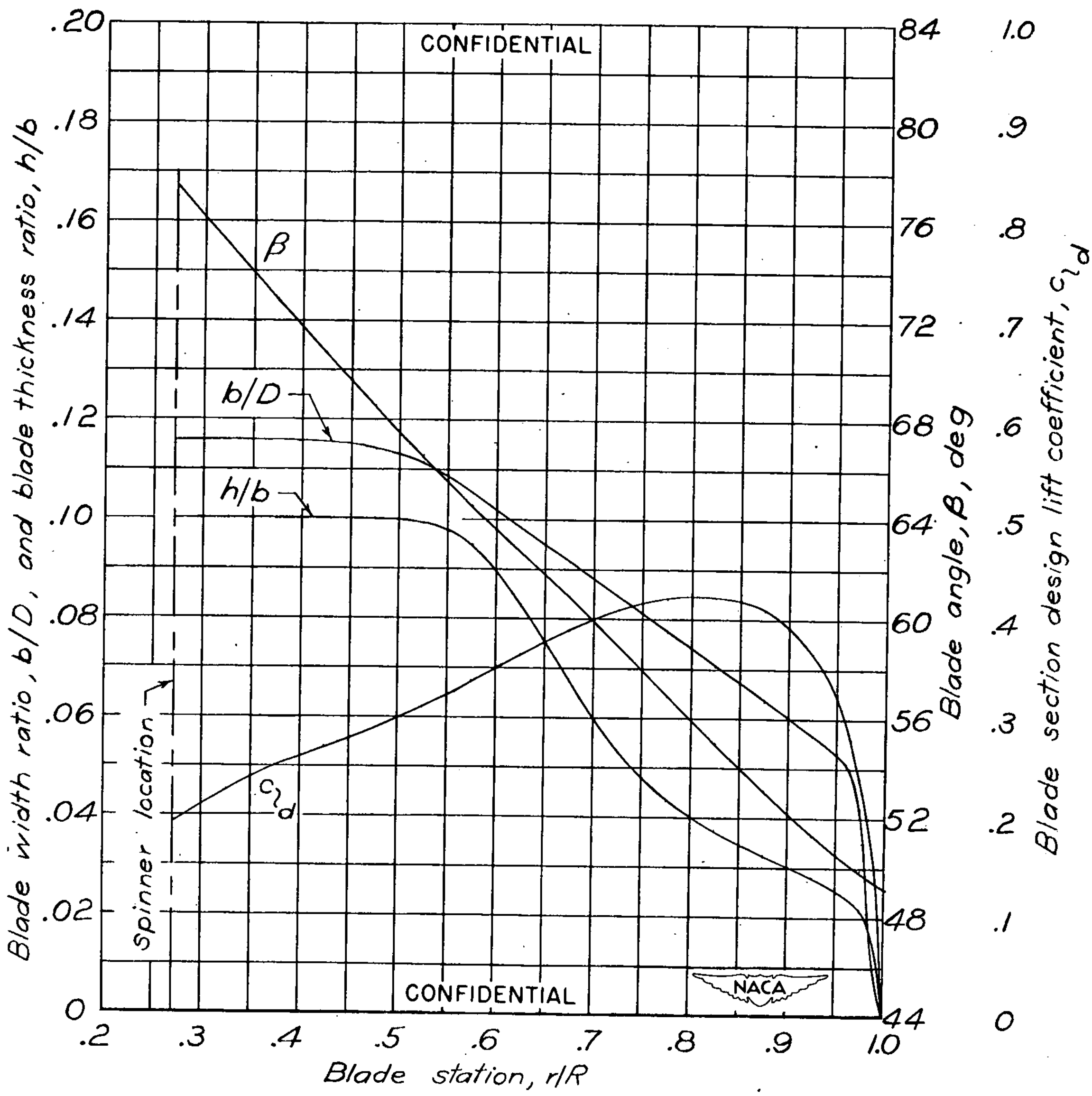

Figure 2.– NACA 4–(4)(06)–04 propeller blade-form curves.

CONFIDENTIAL

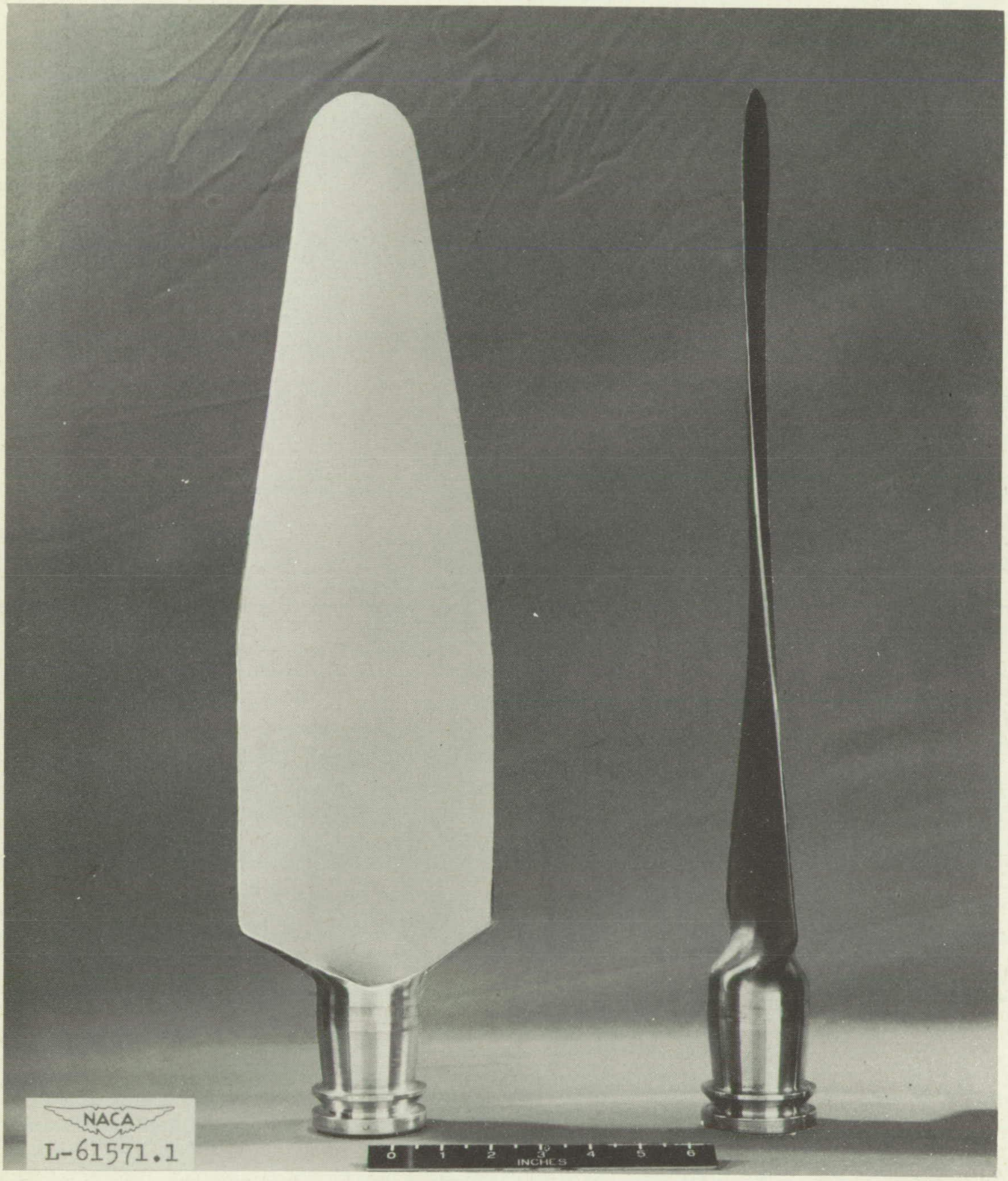

Figure 3.– NACA 4–(4)(06)–04 propeller.

CONFIDENTIAL

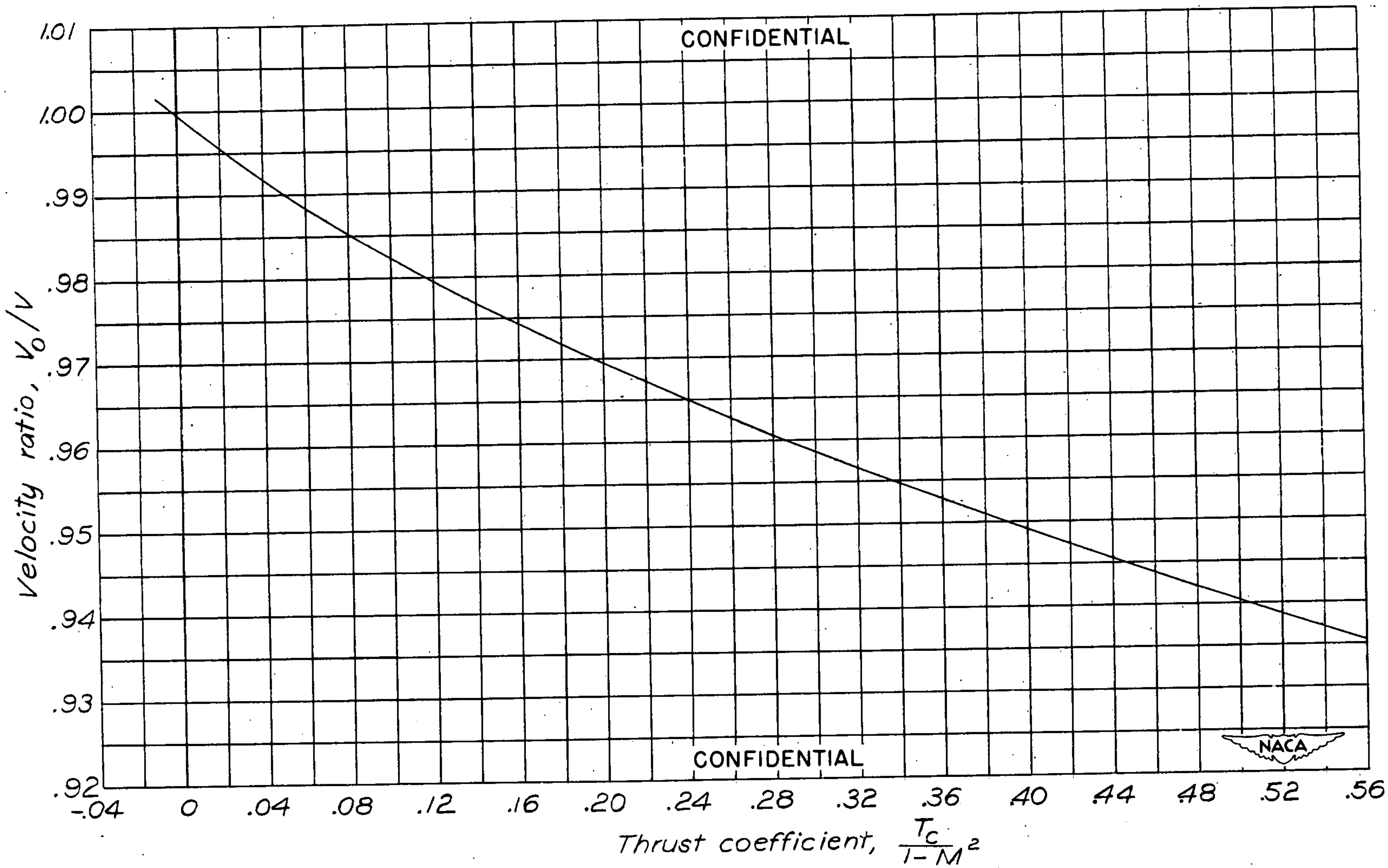

Figure 4.– Tunnel-wall-interference correction for 4-foot-diameter propeller in Langley 8-foot high-speed tunnel.

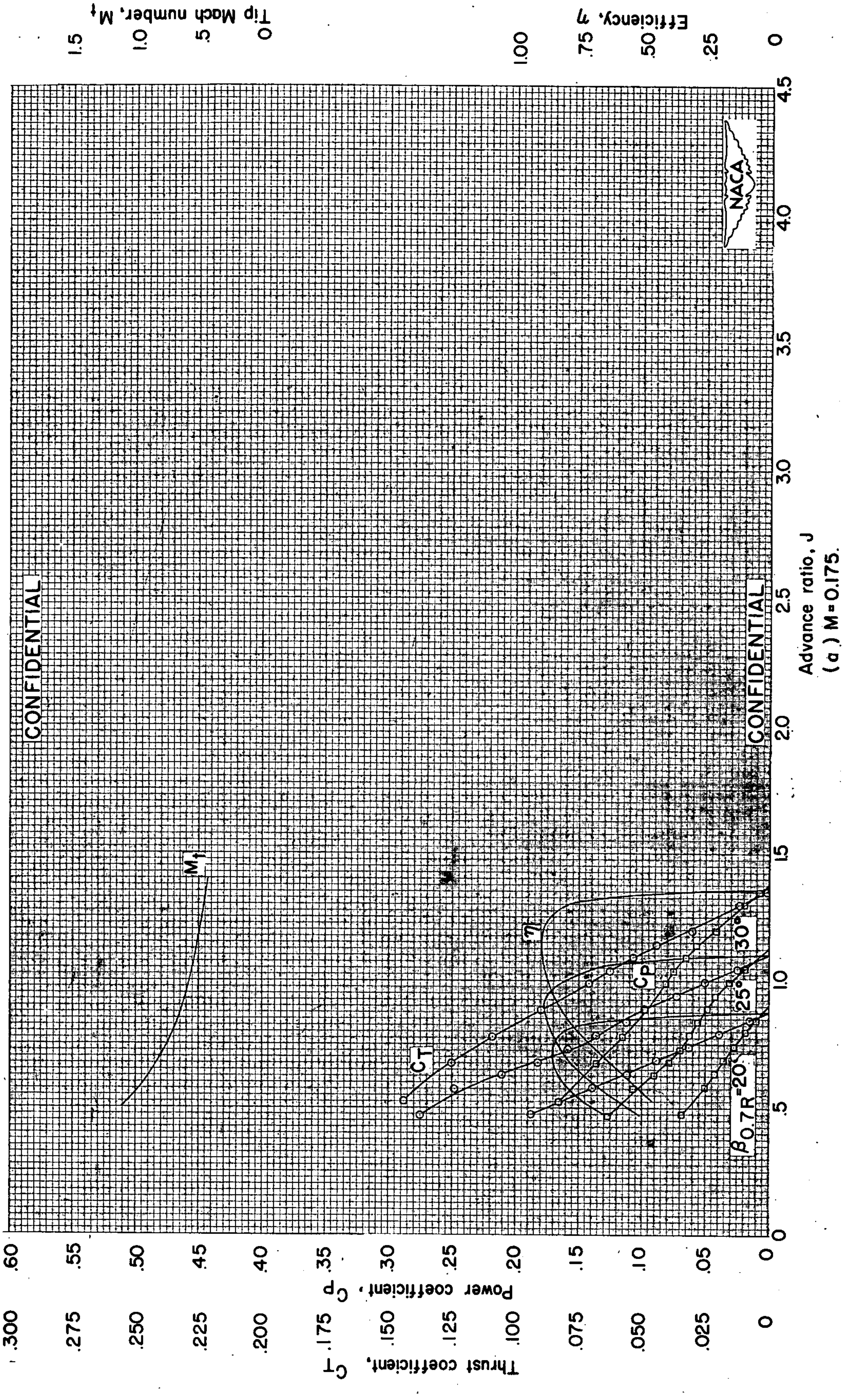

(a) M = 0.175.

Figure 5.- Characteristics of NACA 4-(4)(06)-04 propeller.

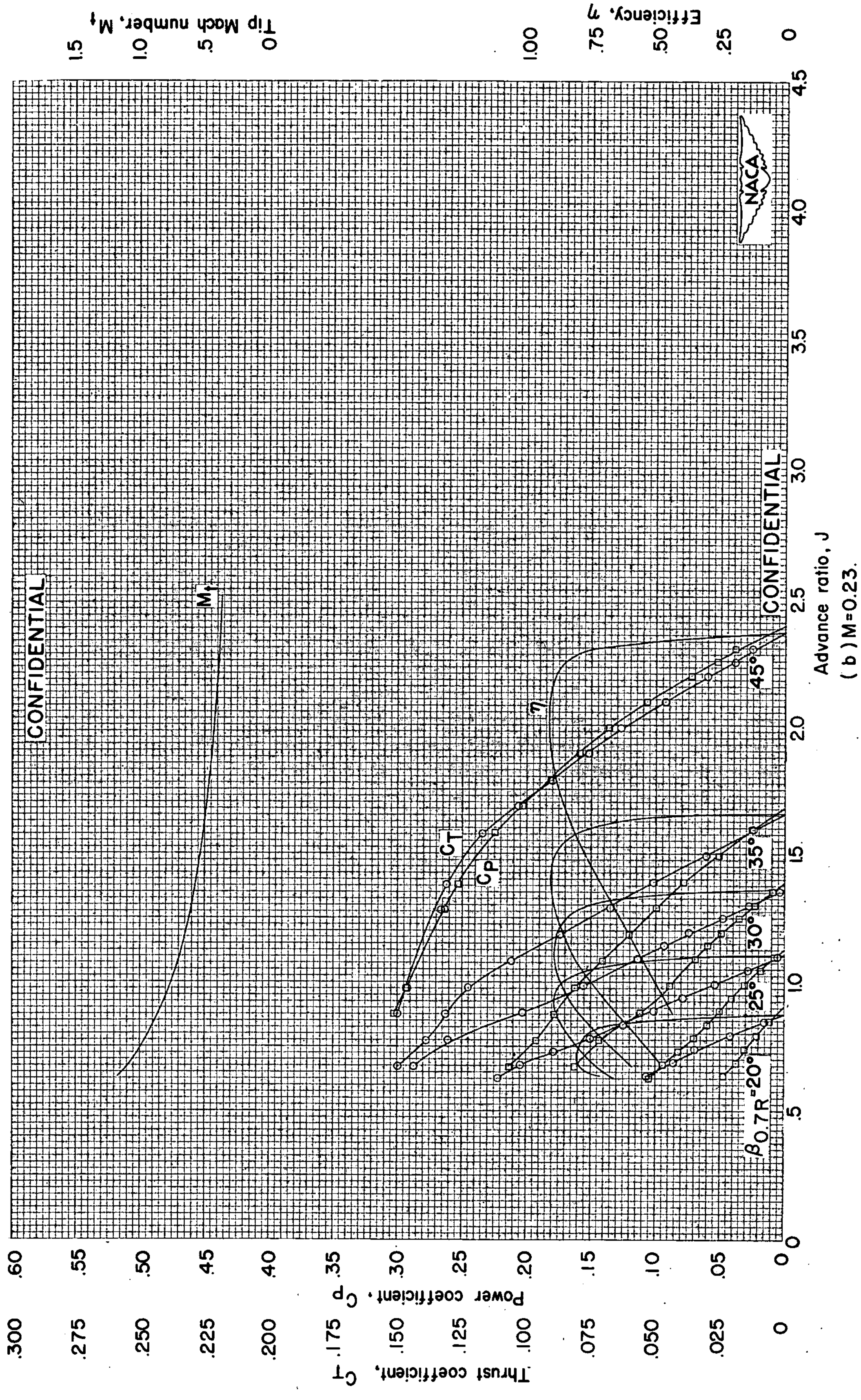

(b) M=0.23.

Figure 5 .- Continued.

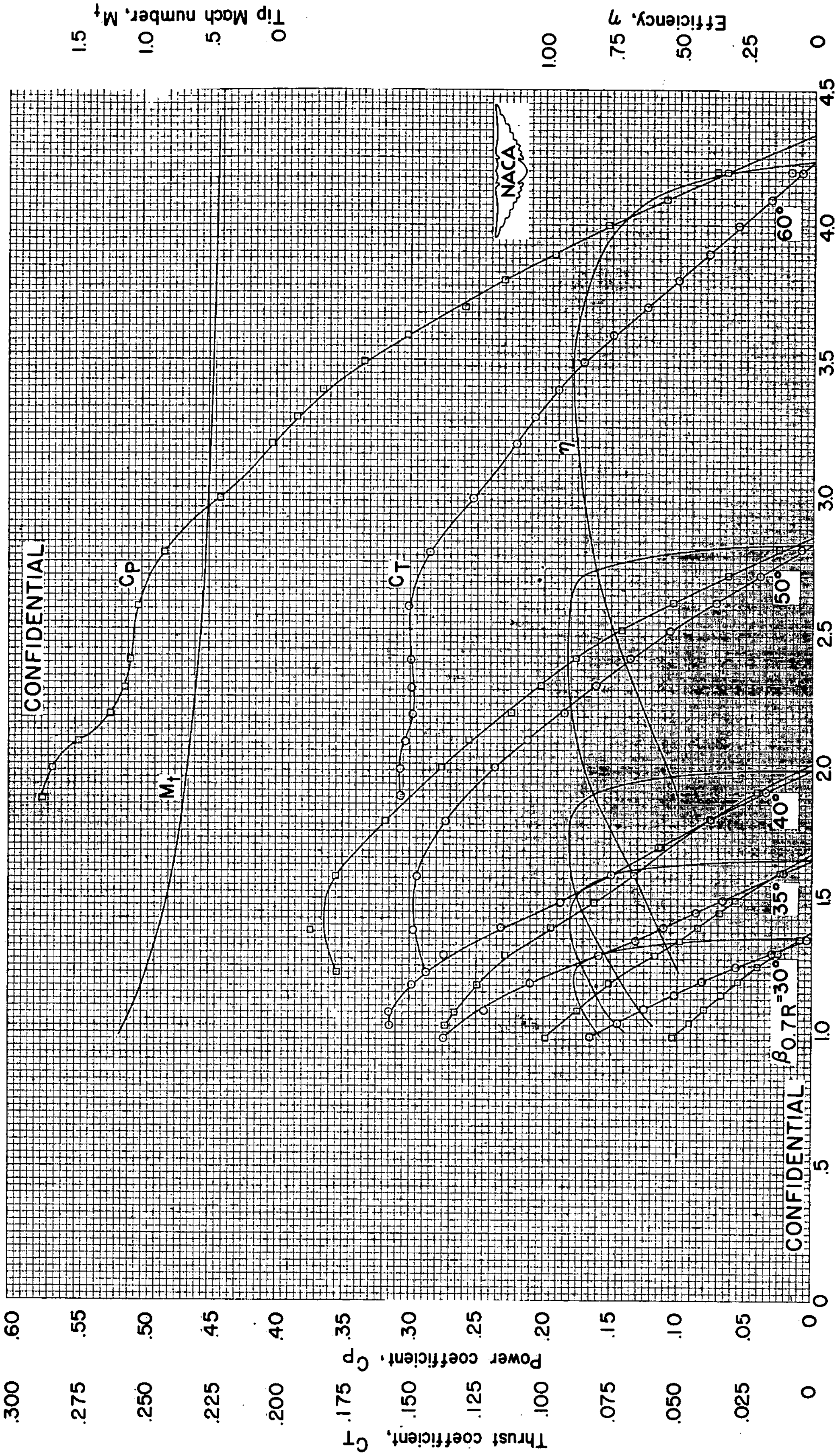

(c) M=0.35.

Figure 5 .- Continued.

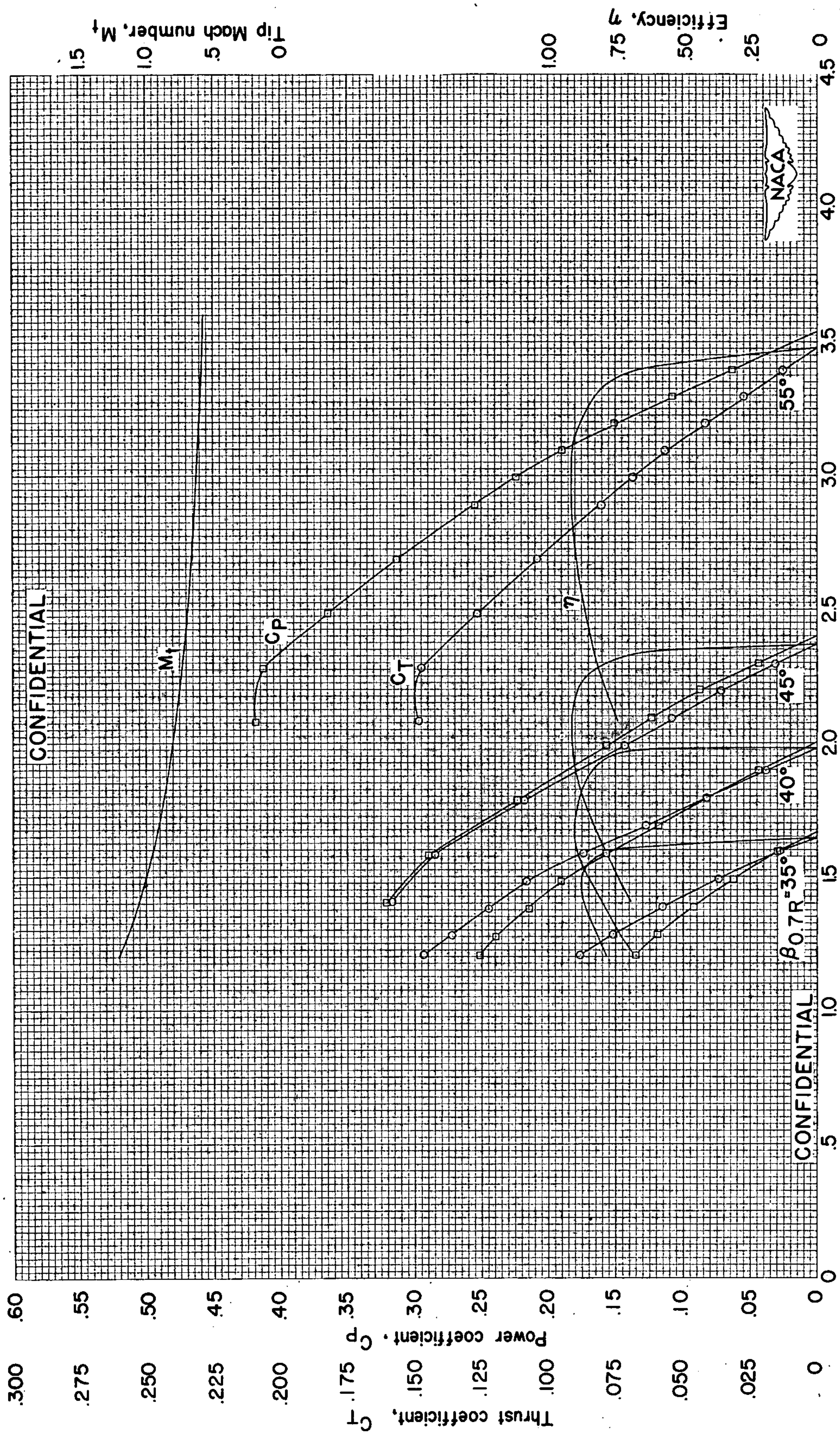

(d) M=0.43.

Figure 5 - Continued.

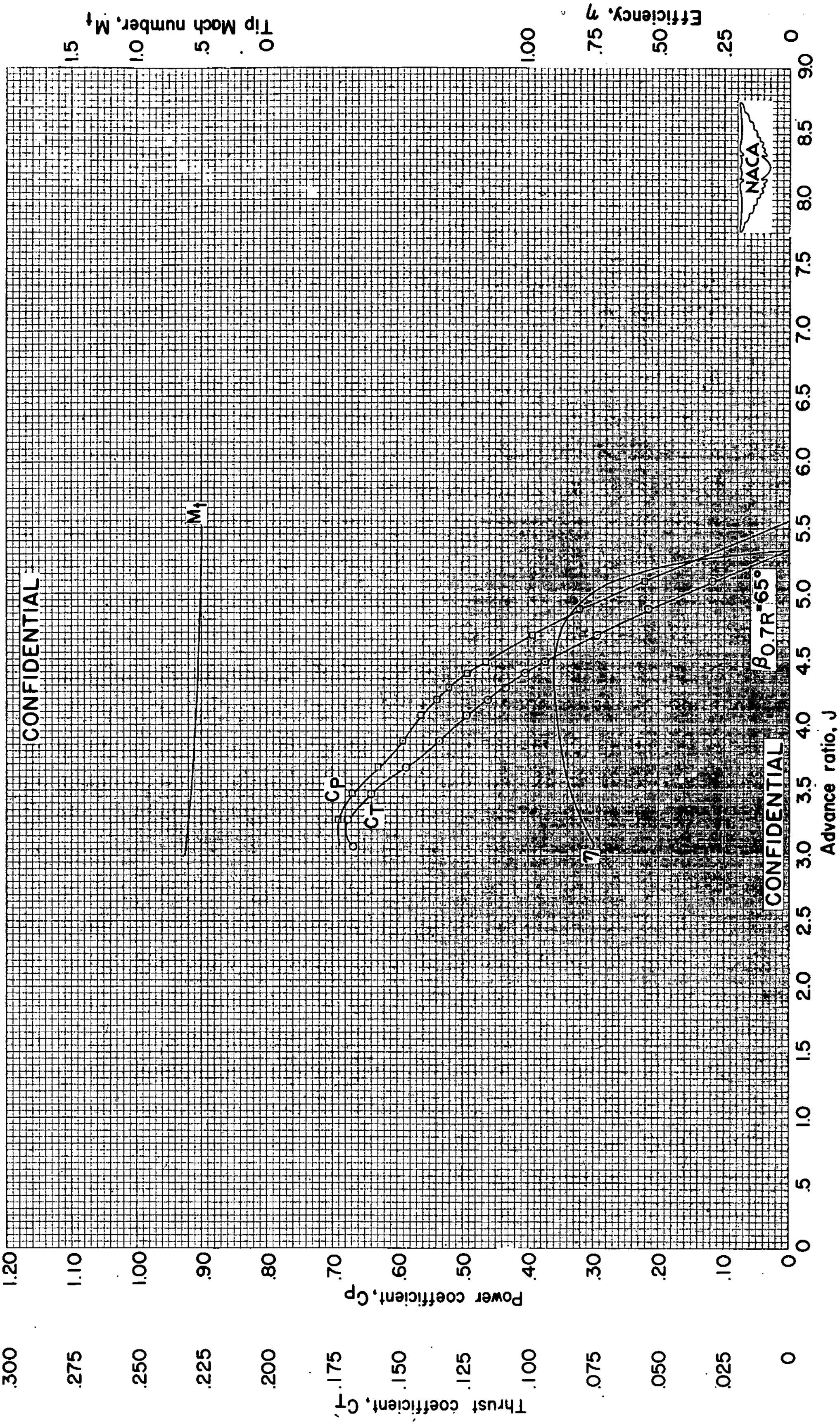

(d) M=0.43. Concluded.

Figure 5 - Continued.

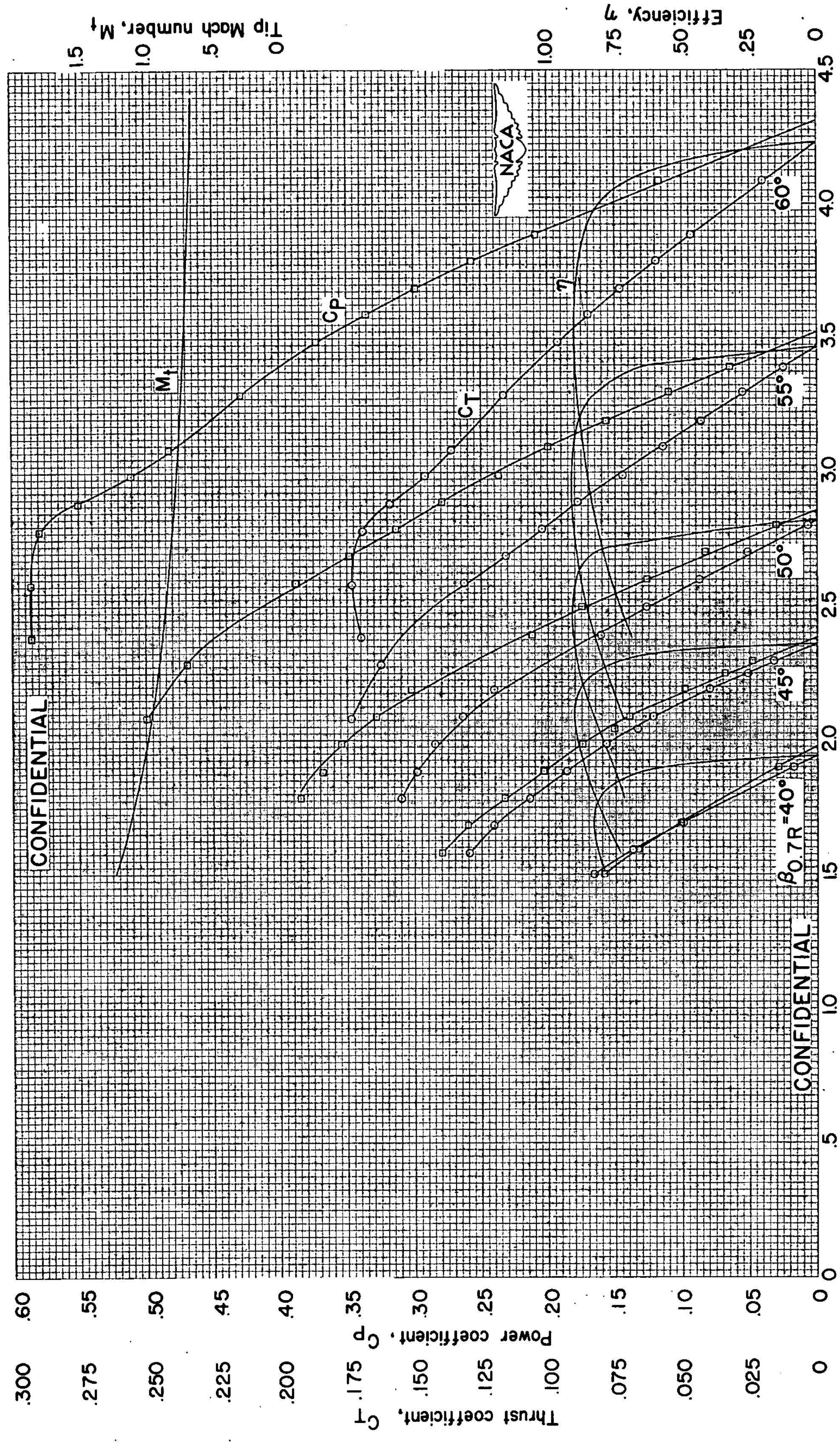

(e) M=0.53.

Figure 5 .- Continued.

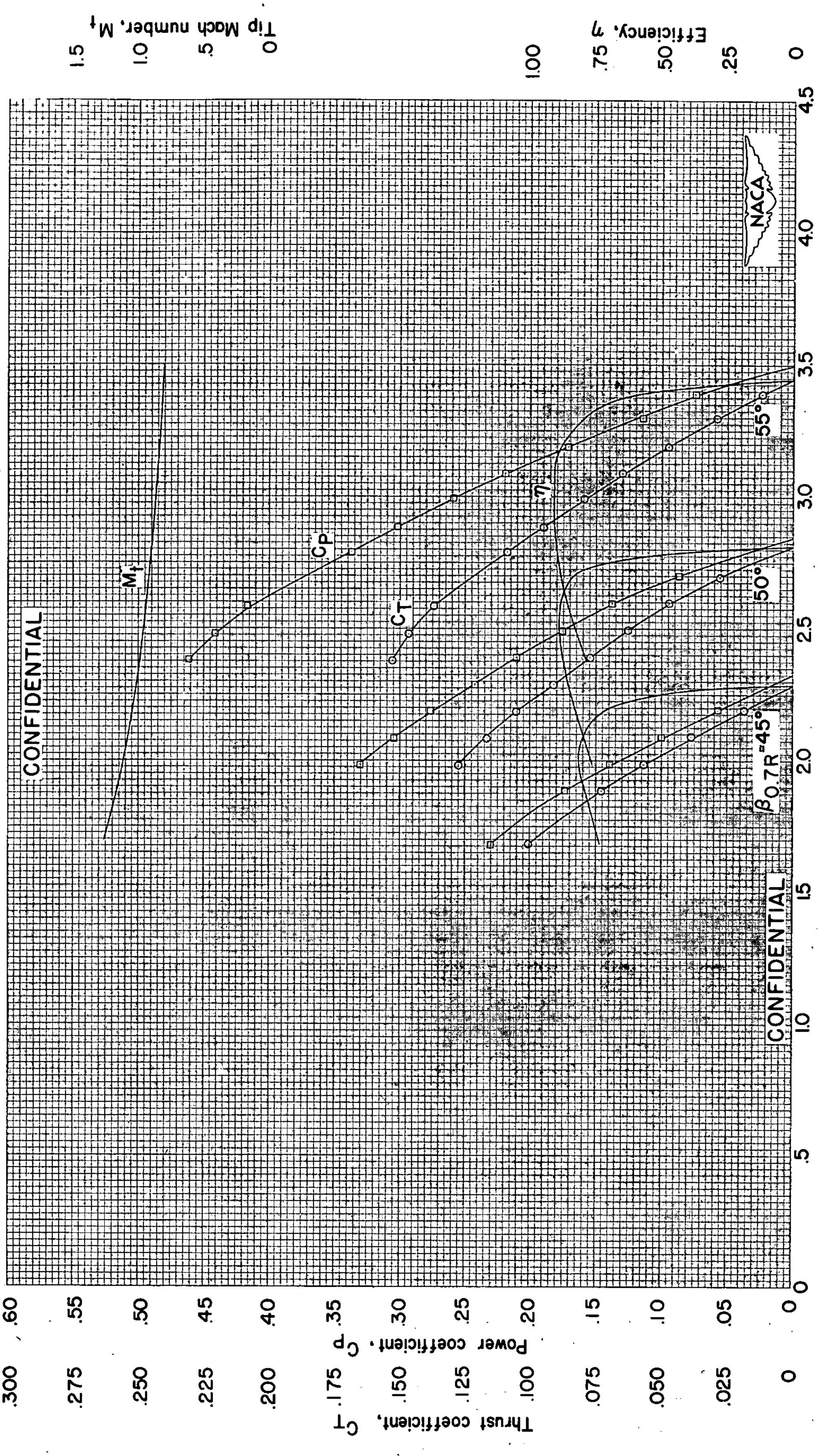

(f) M=0.60.

Figure 5 - Continued.

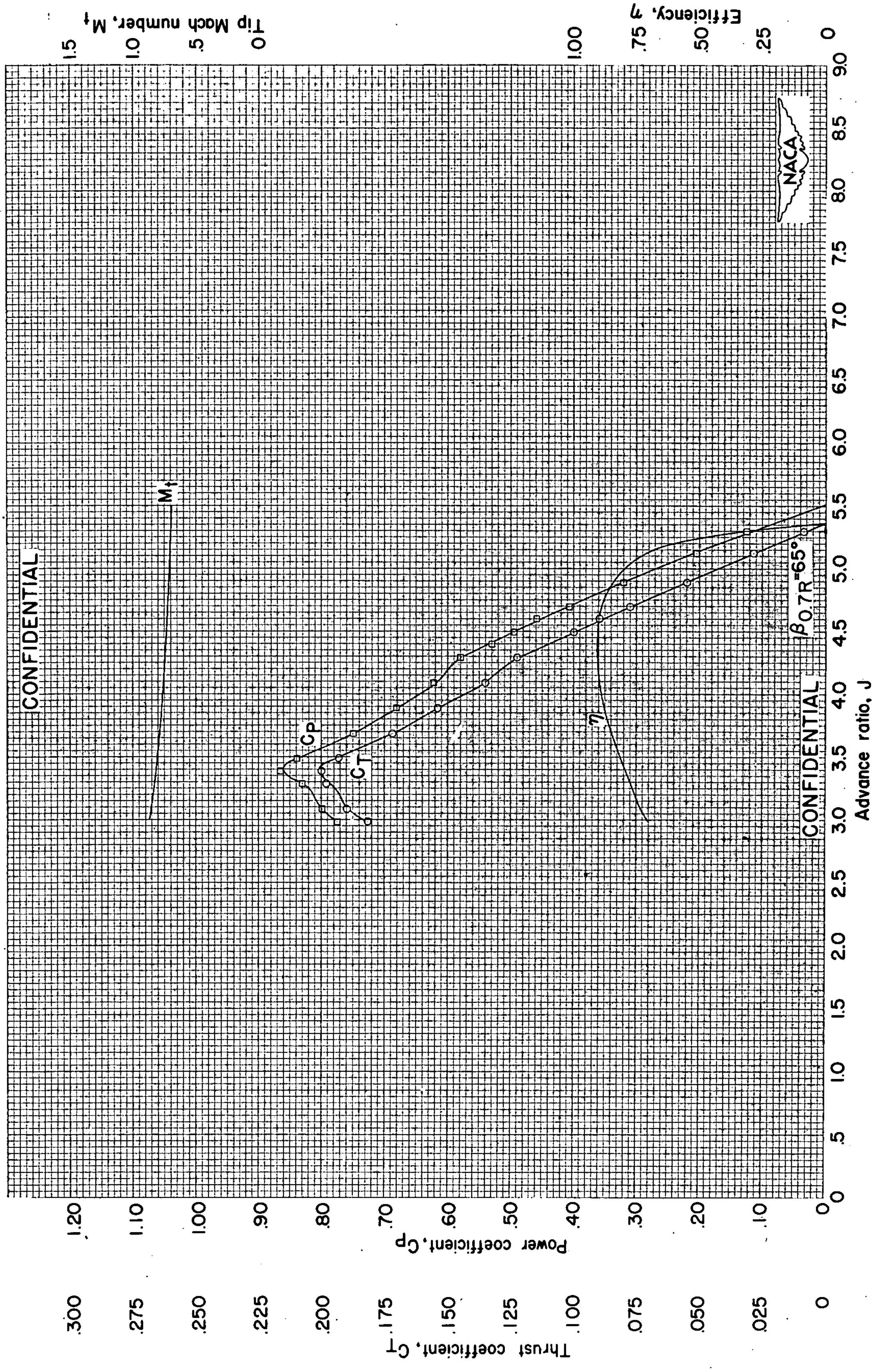

(f) M=0.60. Concluded.

Figure 5.- Continued.

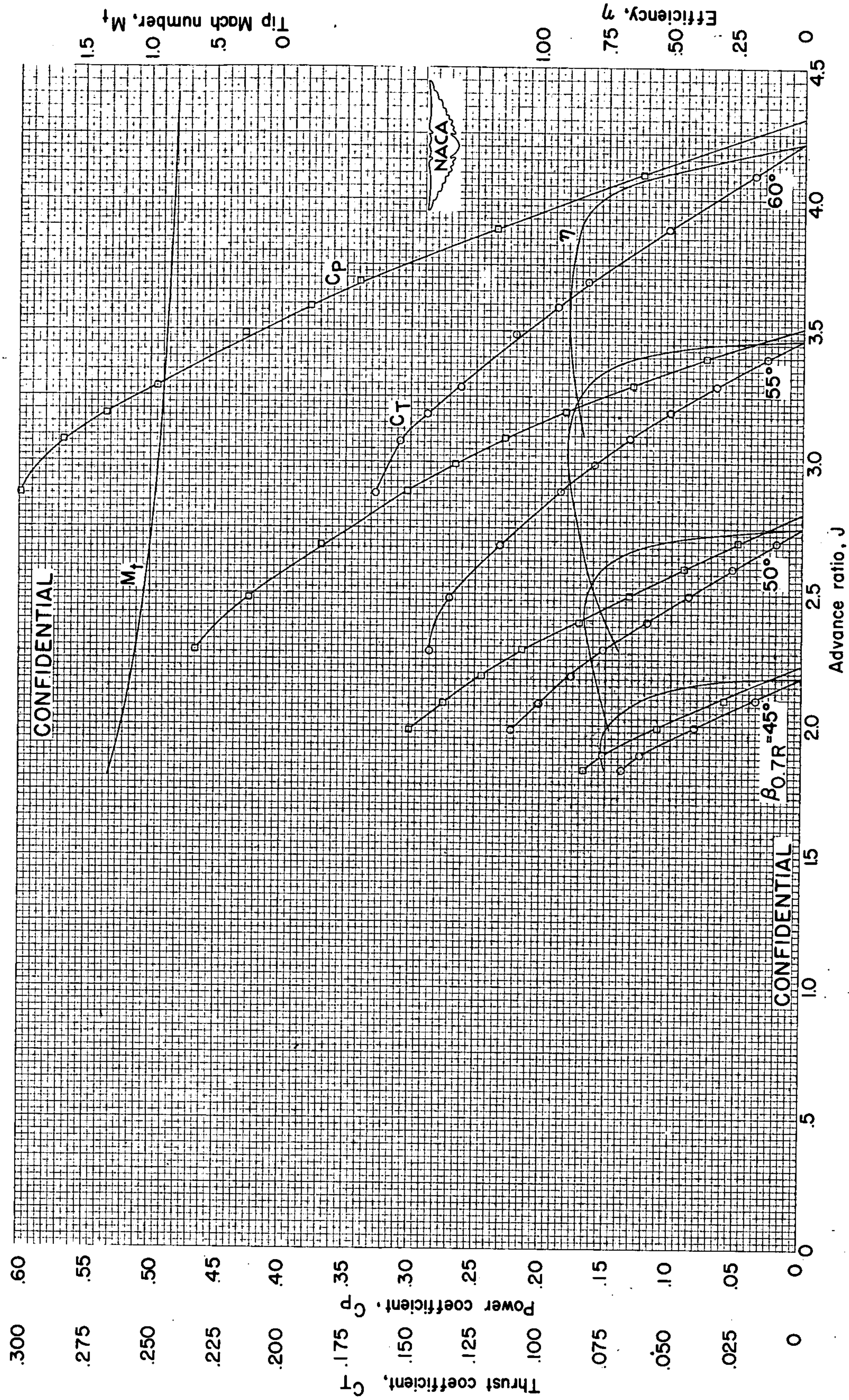

(g) M=0.65.

Figure 5 - Continued.

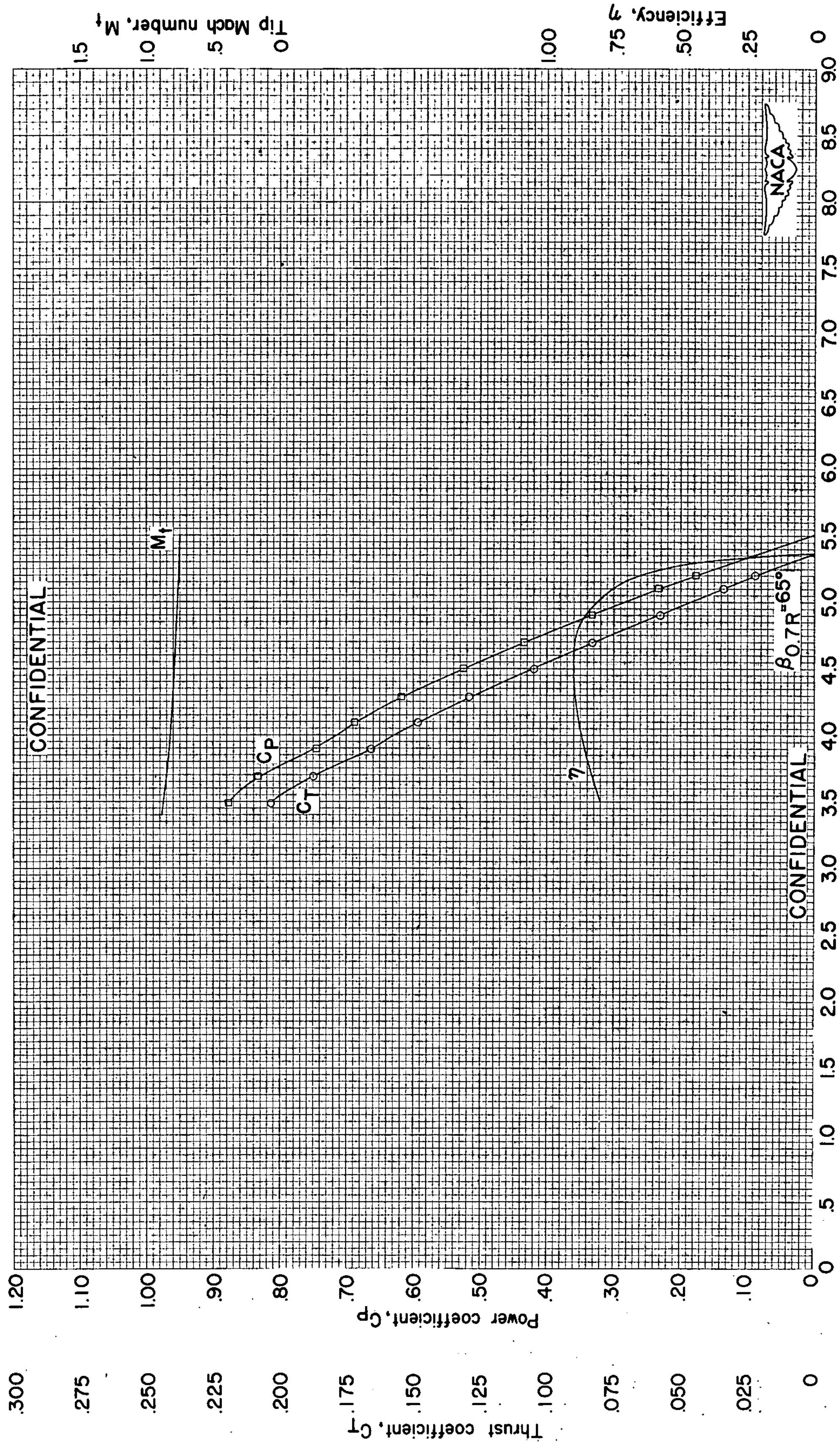

(g) M=0.65. Concluded.

Figure 5 - Continued.

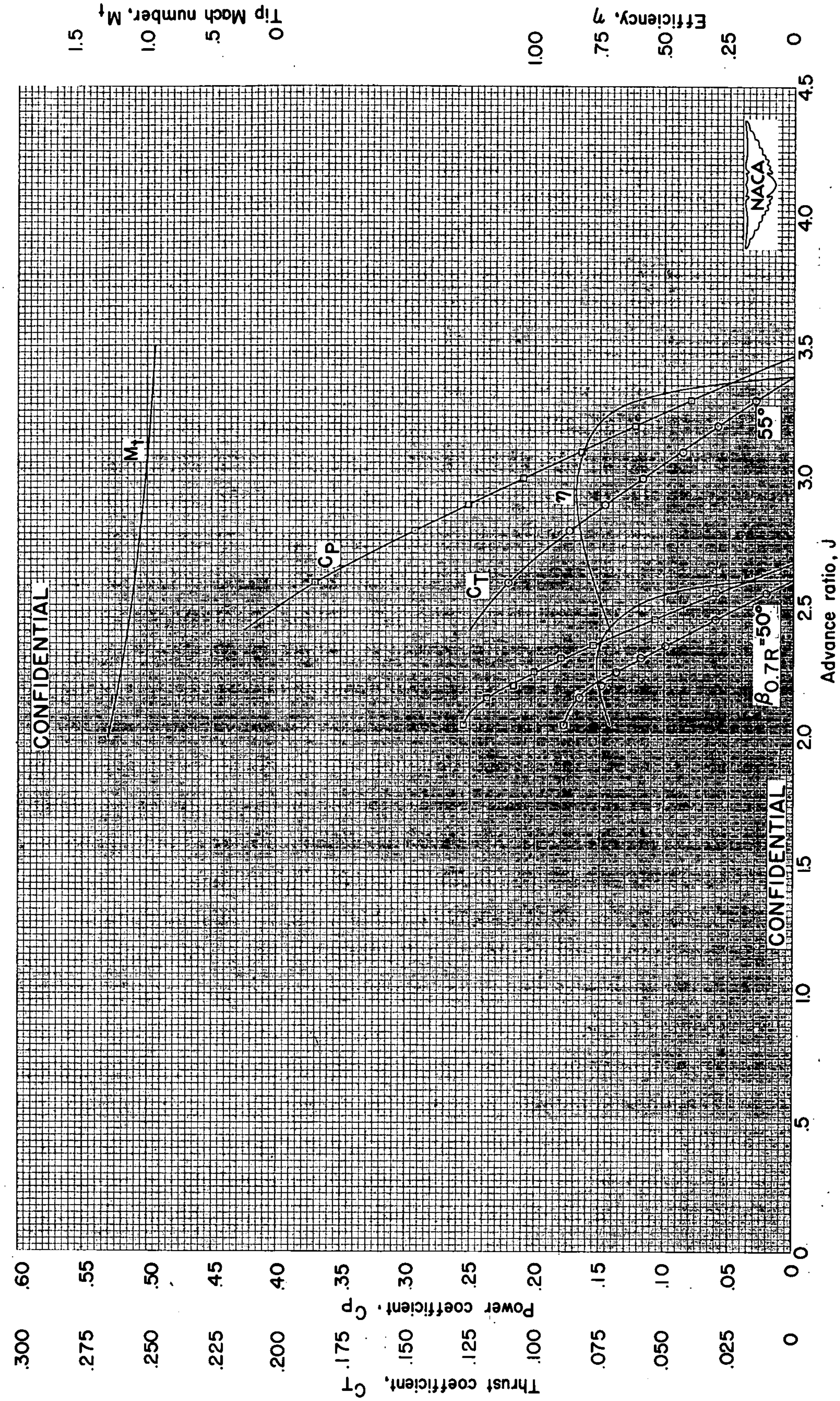

(h) M=0.70.

Figure 5 .- Continued.

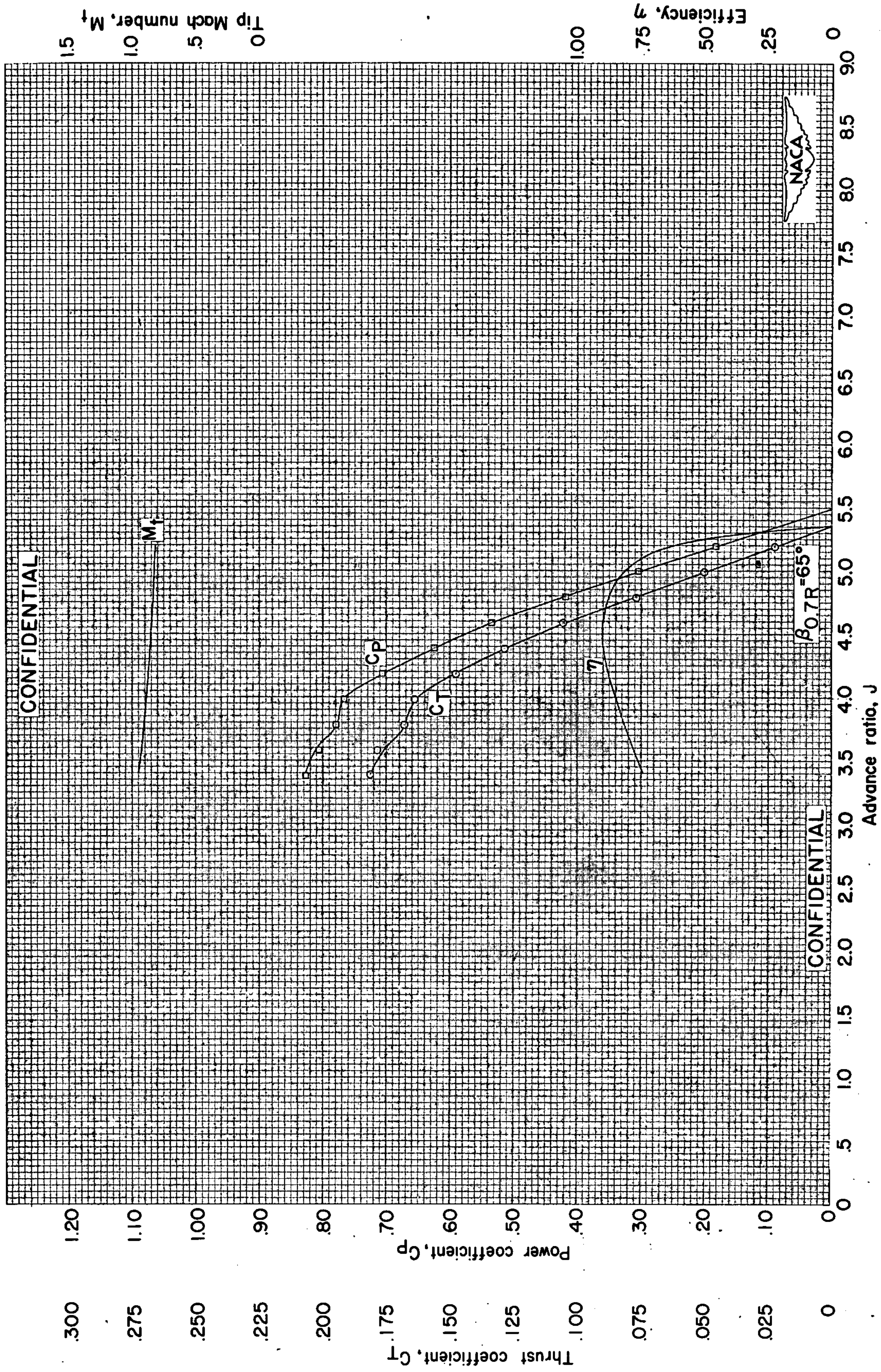

(h) M=0.70. Concluded.

Figure 5 - Continued.

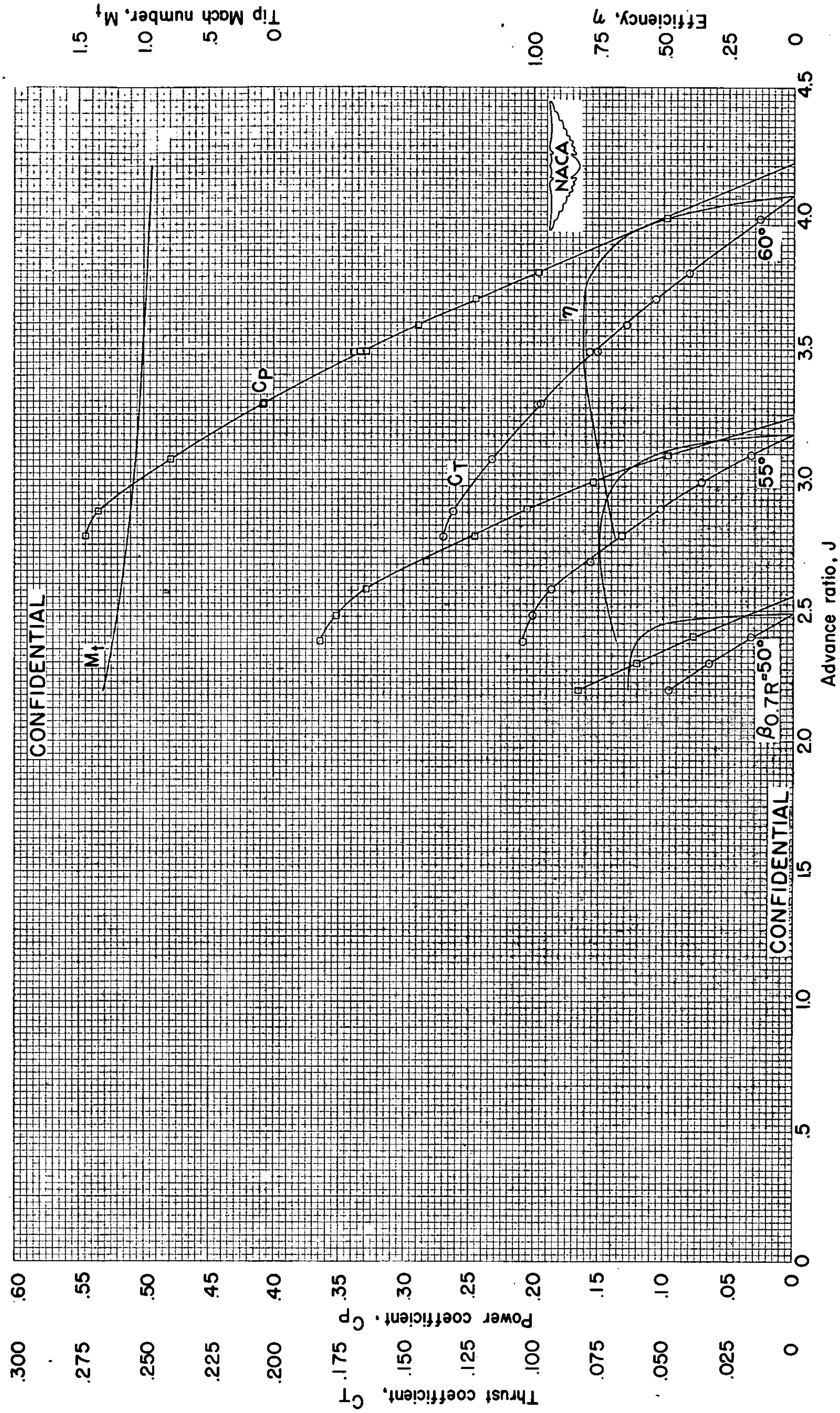

(i) M=0.75

Figure 5 .- Continued.

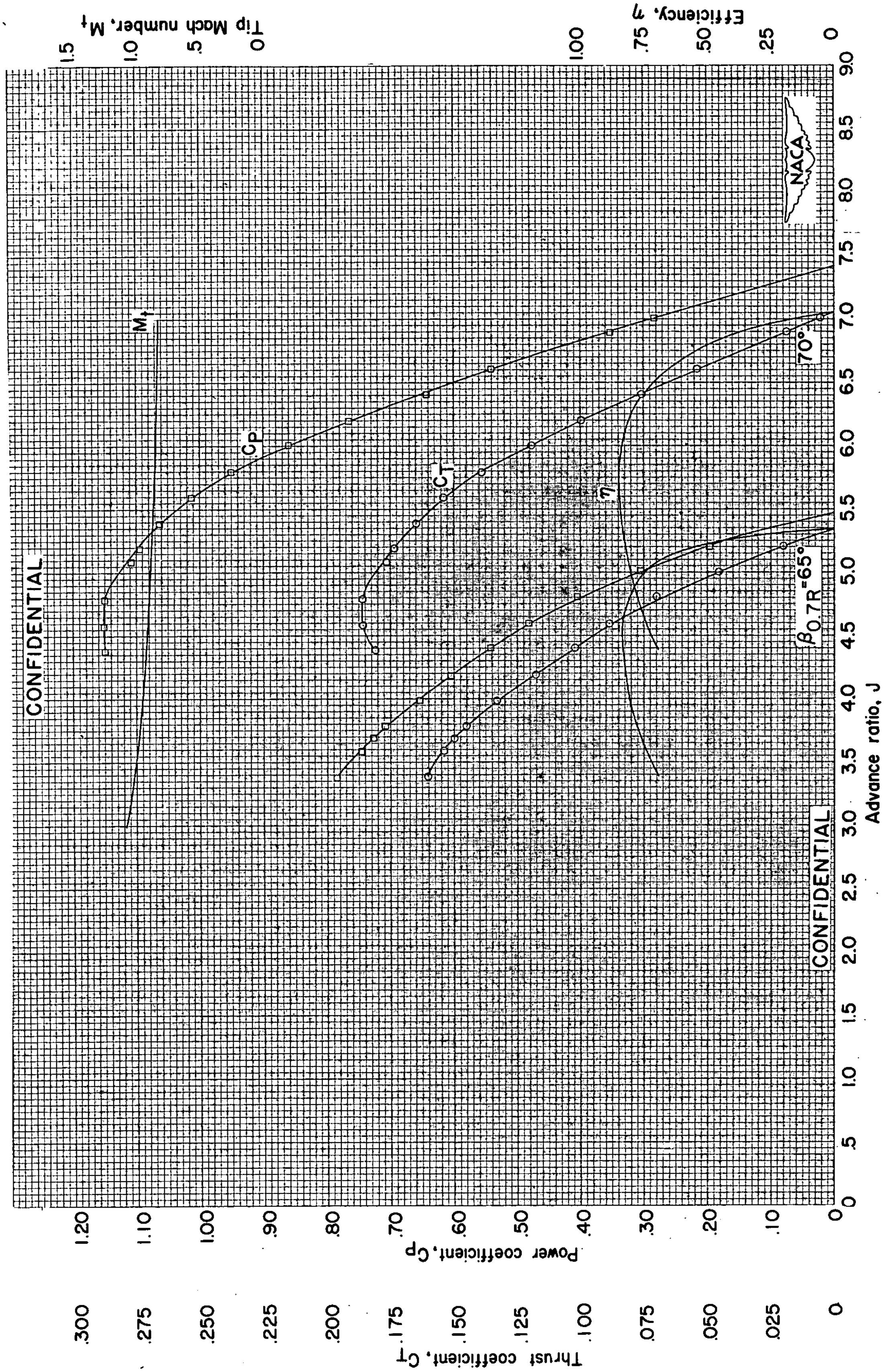

(i) M=0.75. Concluded.

Figure 5 .- Continued.

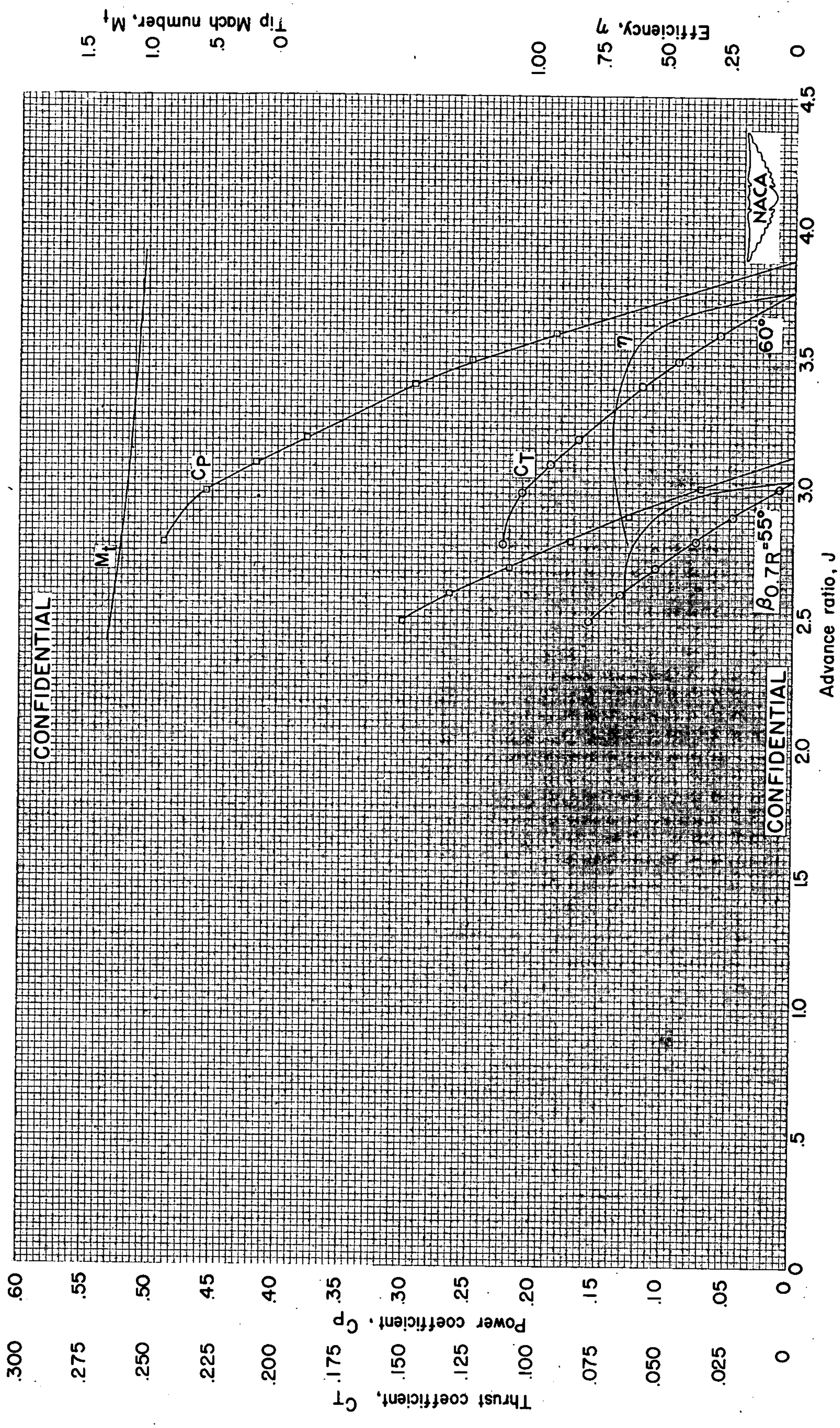

(j) M=0.80.

Figure 5 .- Continued.

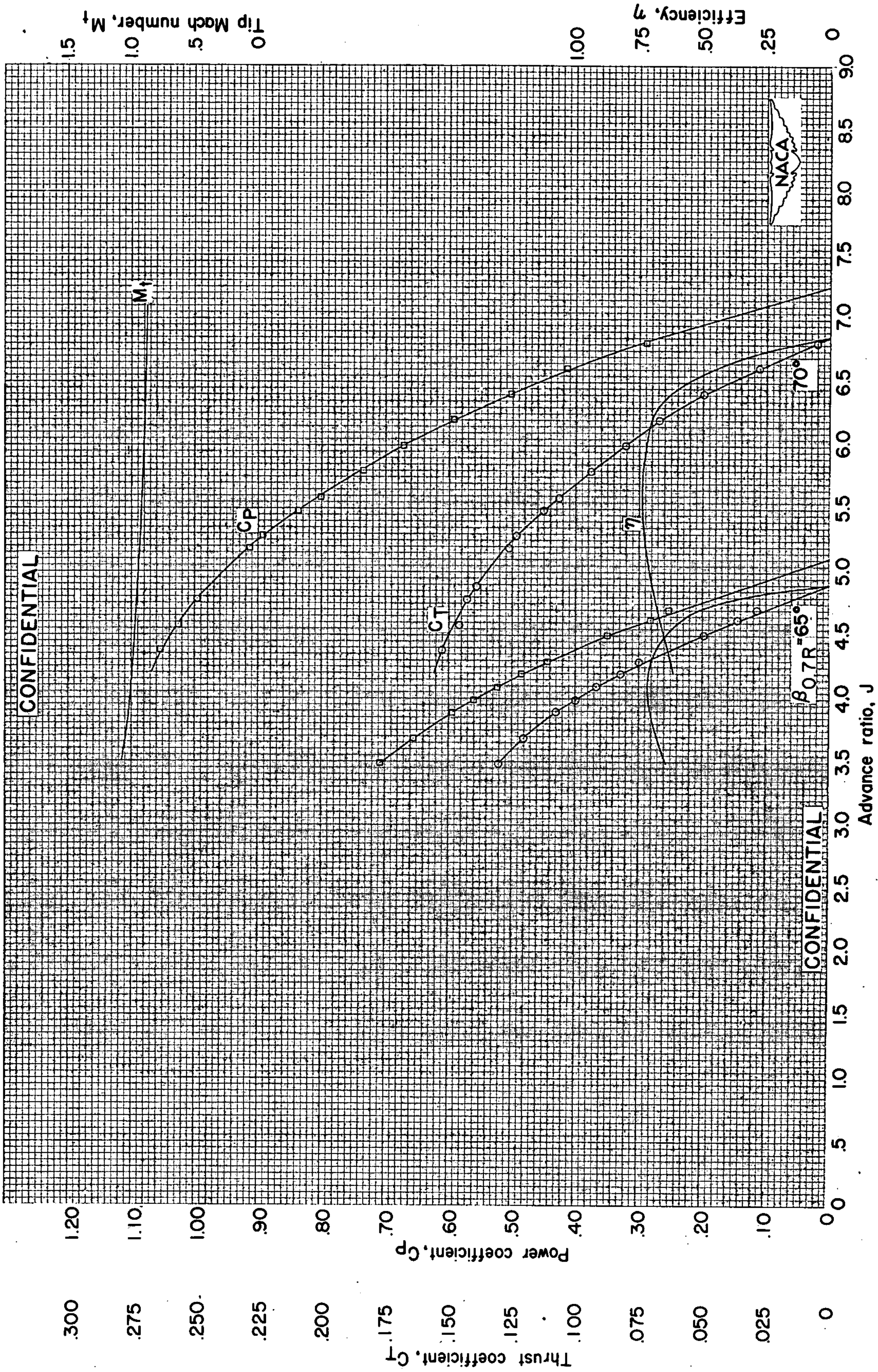

(j) M=0.80. Concluded.

Figure 5 .- Continued.

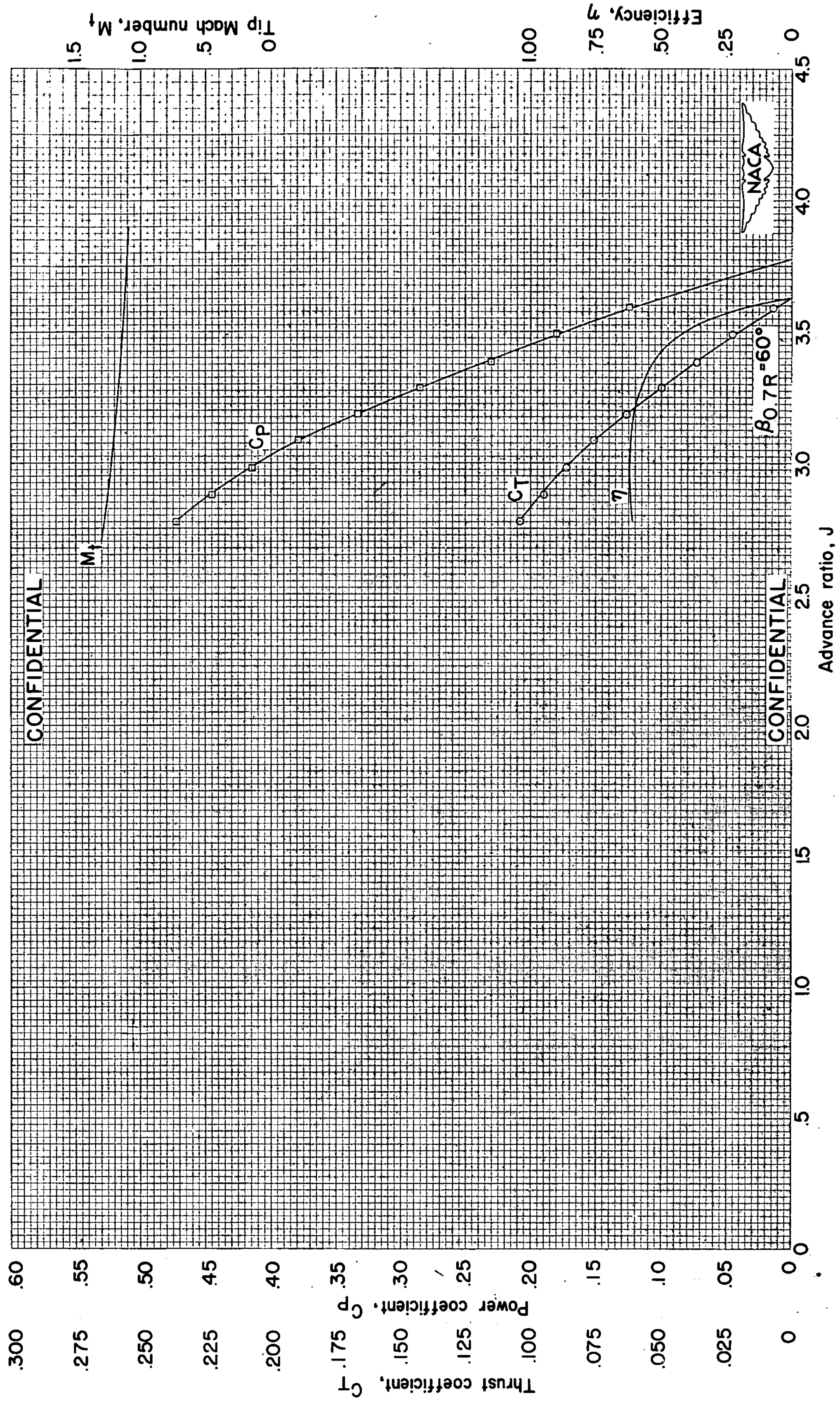

(k) M=0.85.

Figure 5.- Continued.

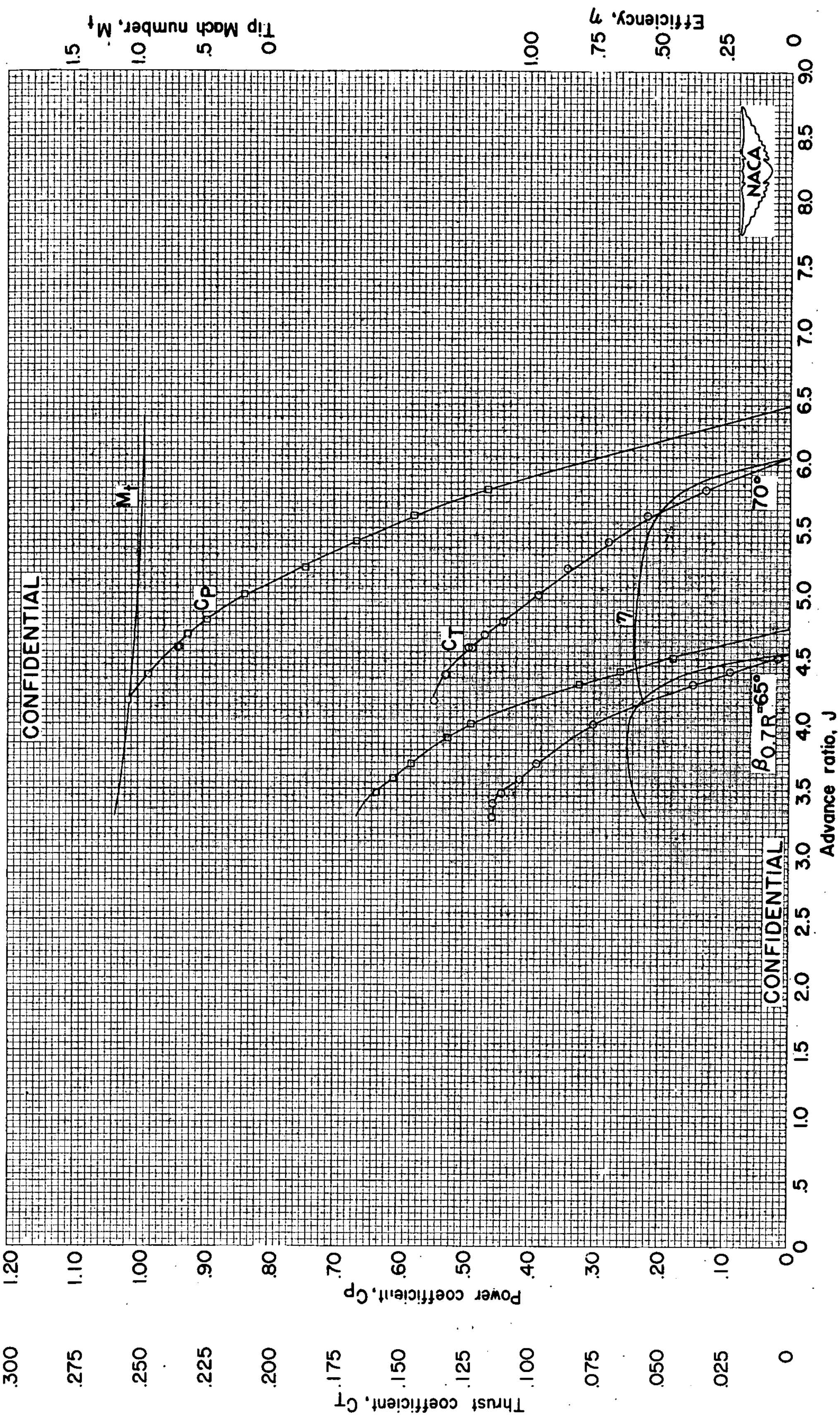

(k) M=0.85. Concluded.

Figure 5 - Continued.

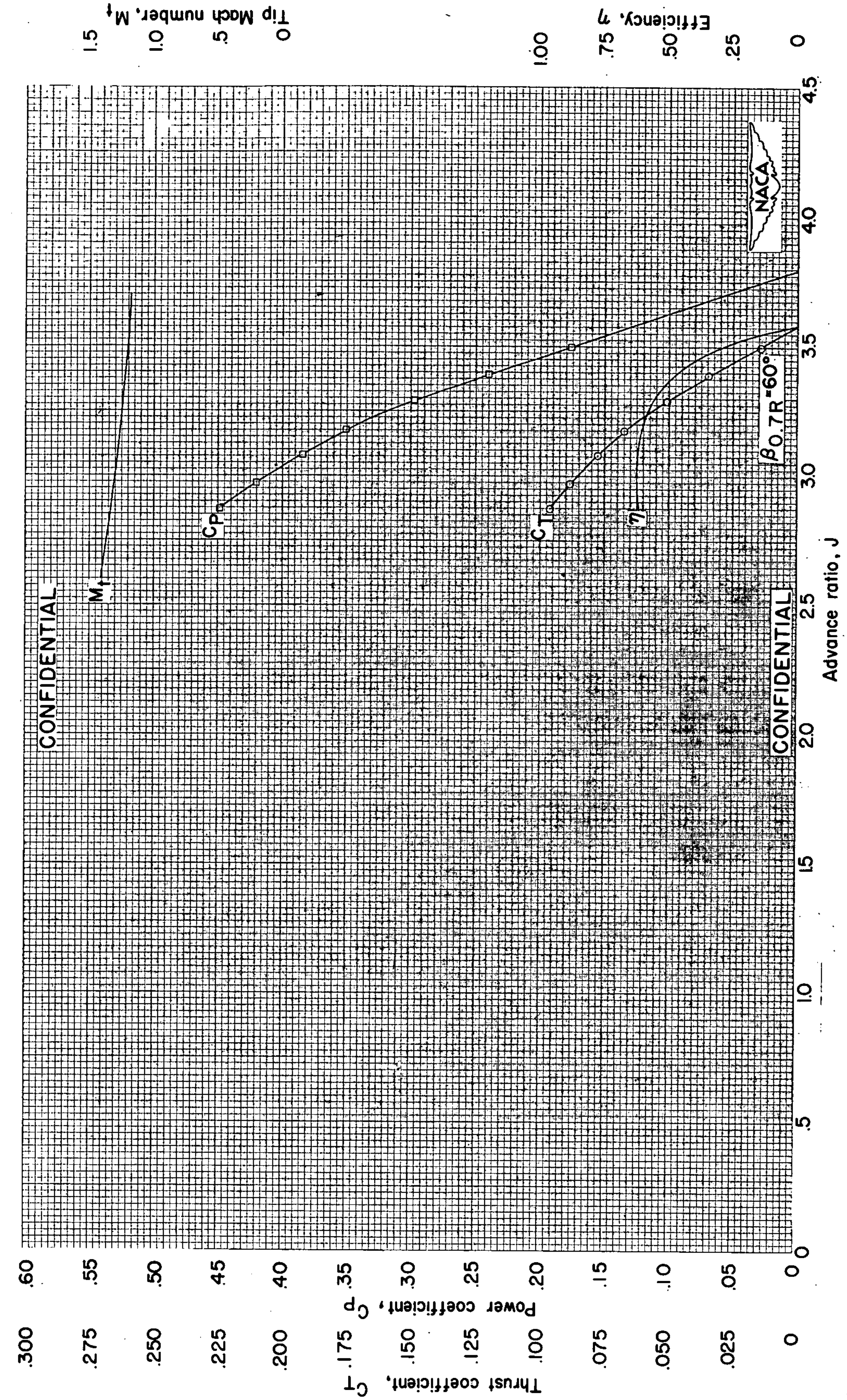

(l) M=0.90.

Figure 5 .- Continued.

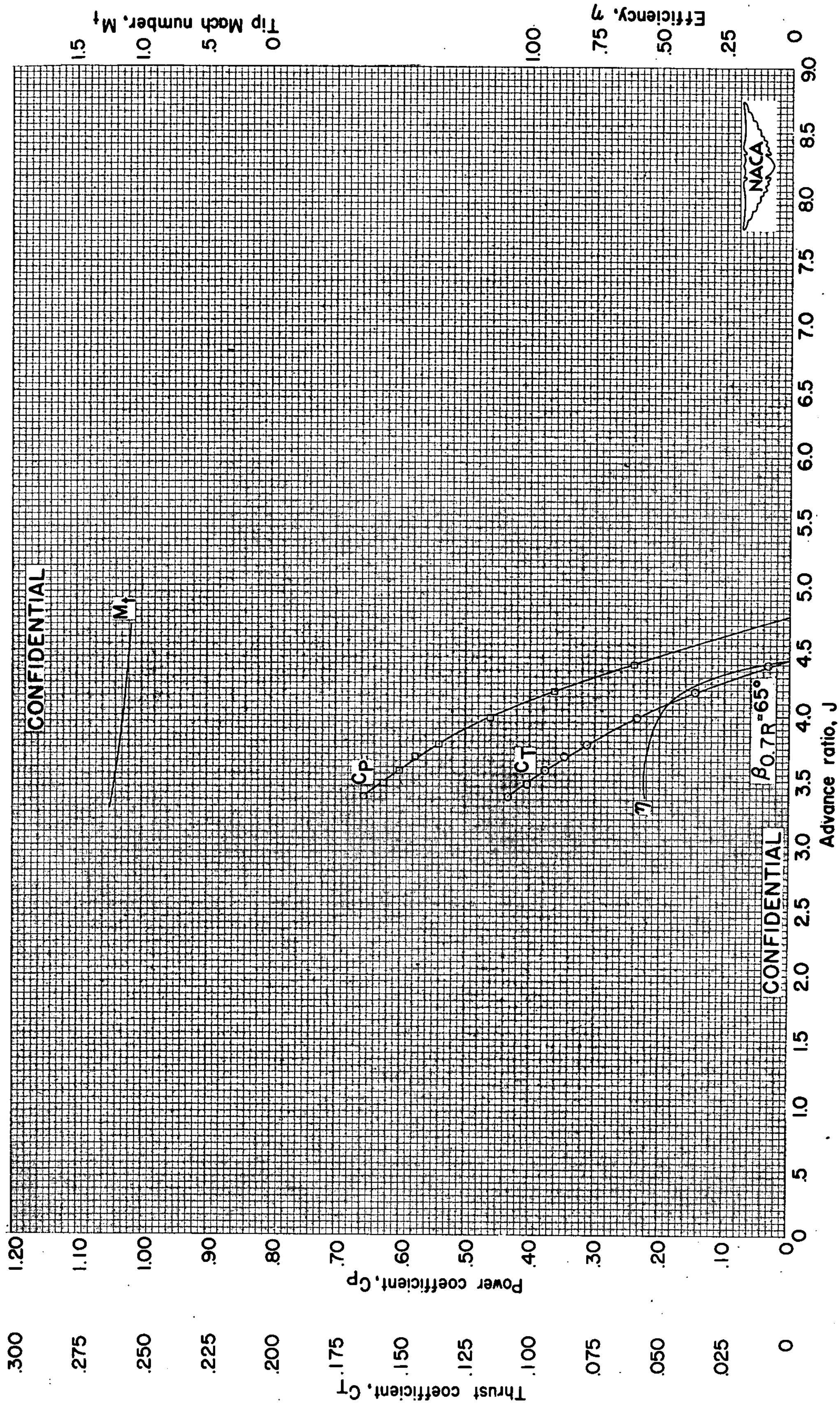

(l) M=0.90. Concluded.

Figure 5 - Continued.

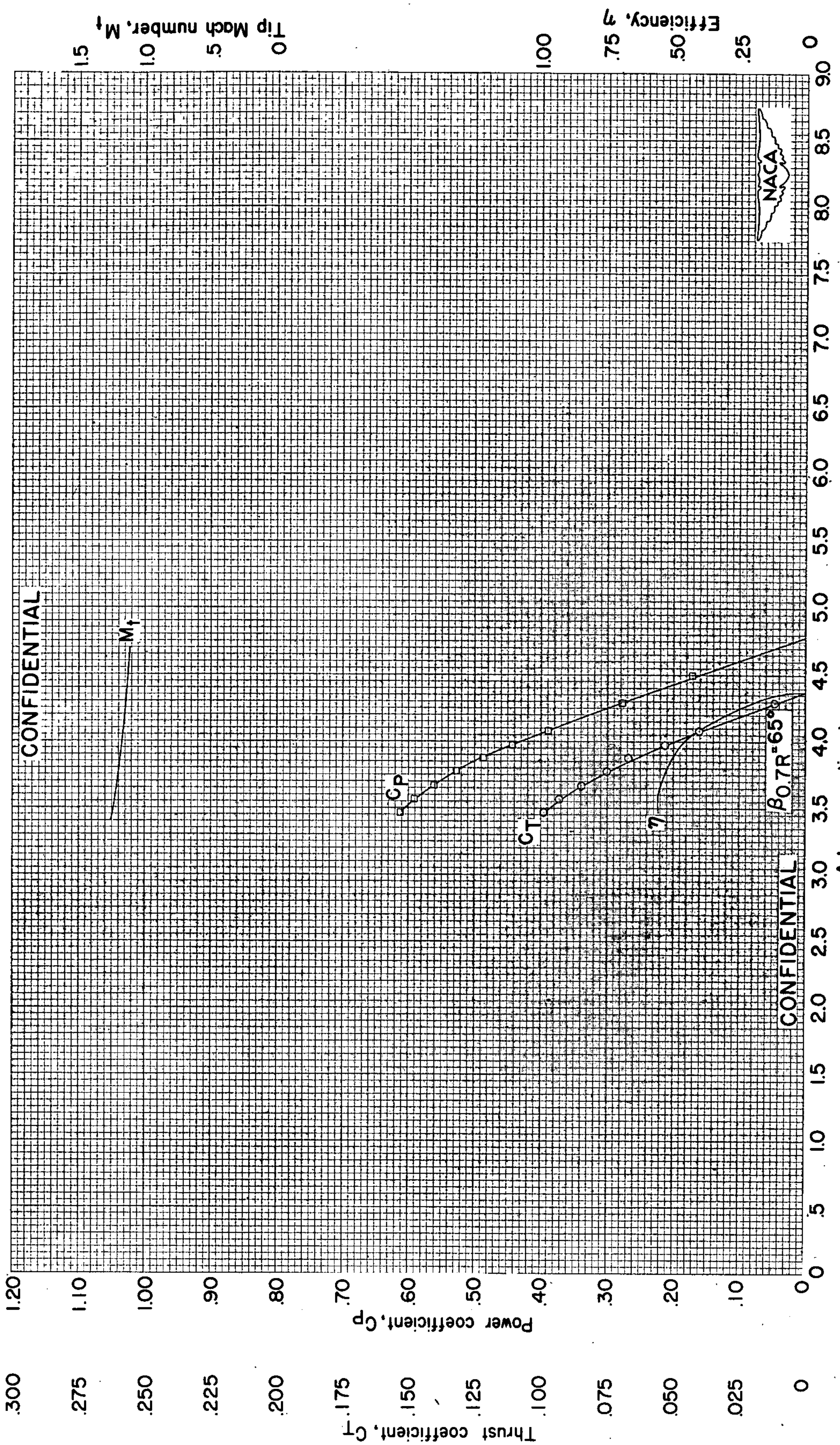

(m) M=0.925.

Figure 5 .- Concluded.

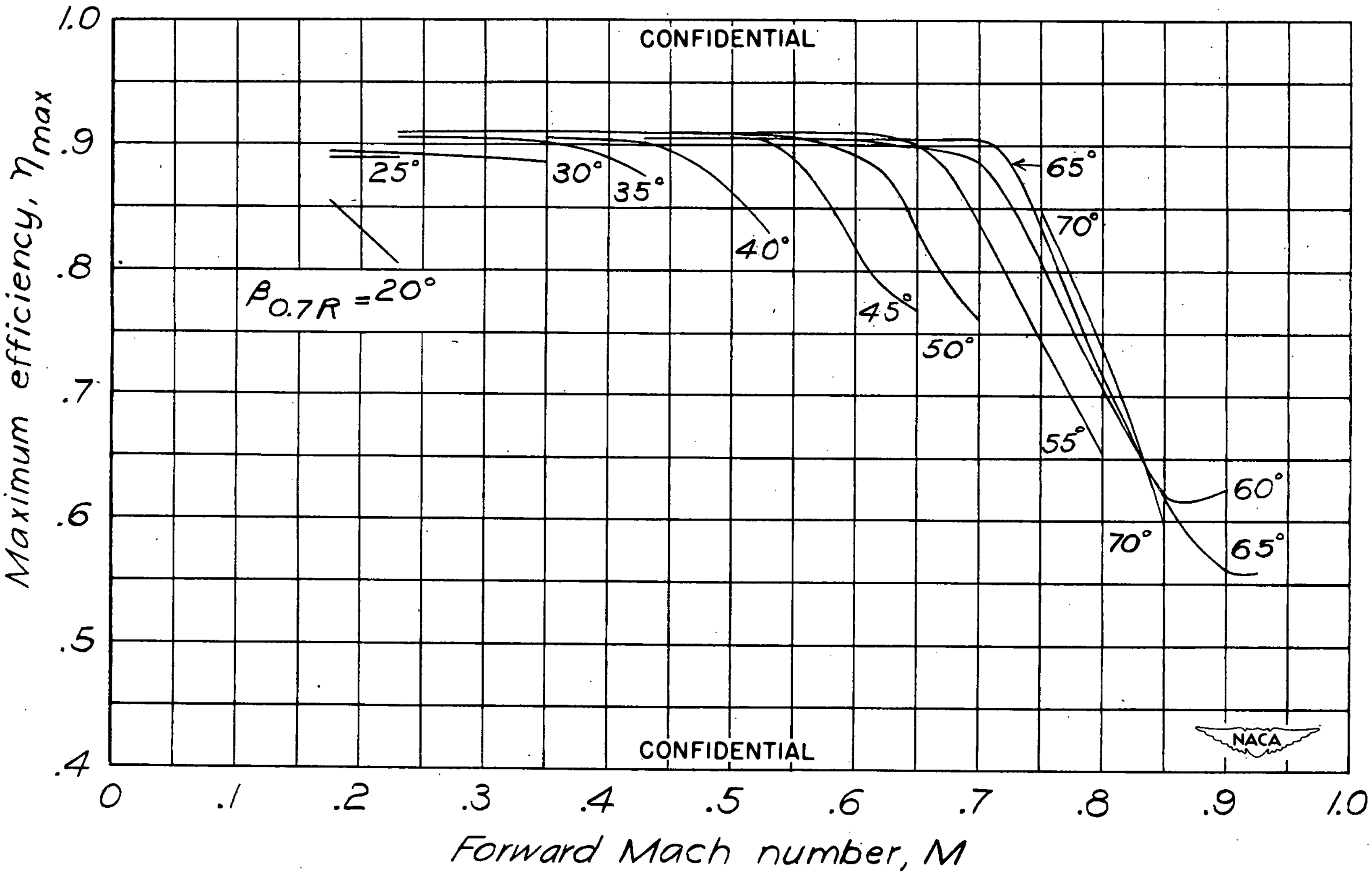

Figure 6.– Effect of forward Mach number on maximum efficiency.

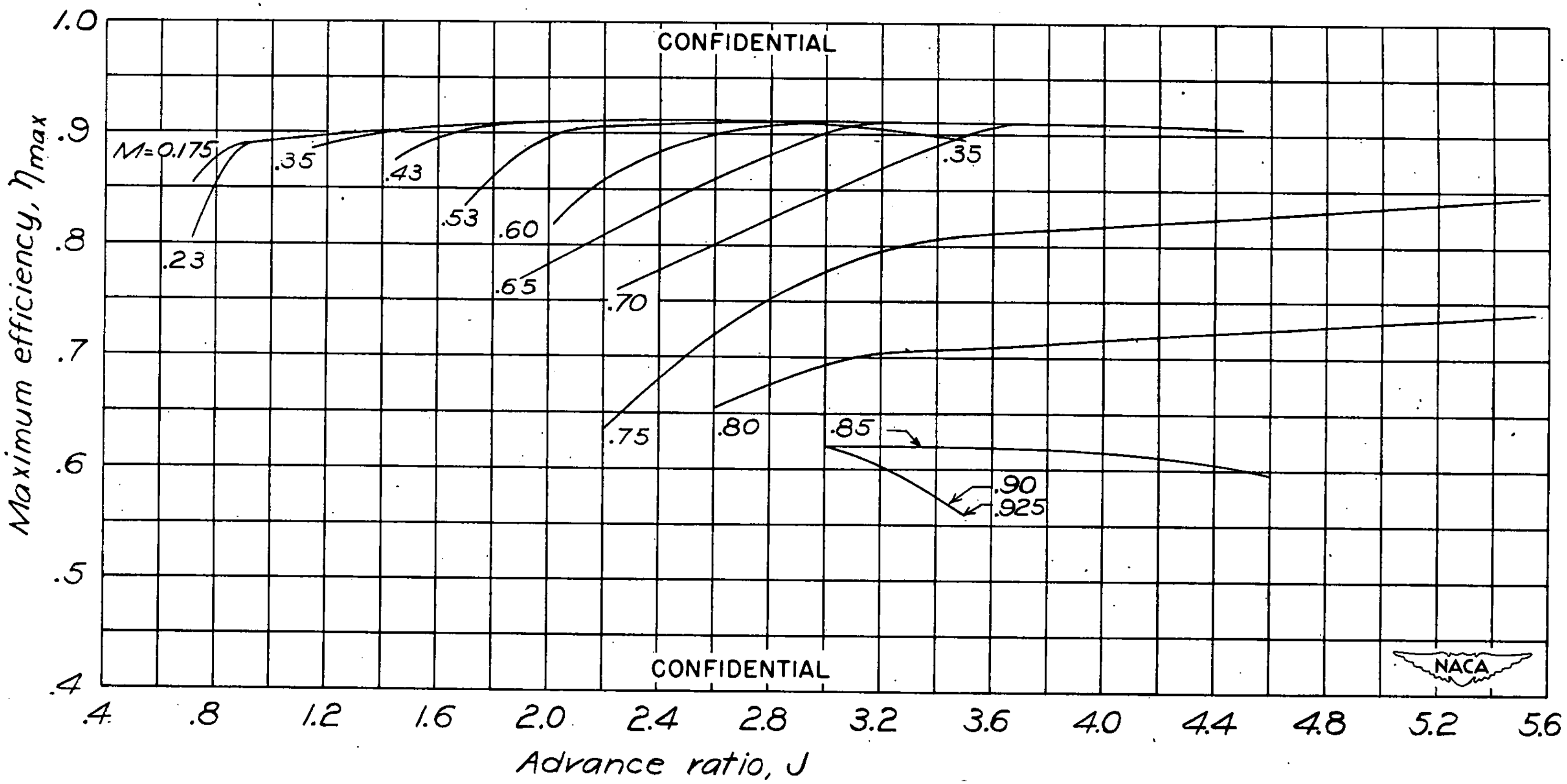

Figure 7.– Effect of forward Mach number and advance ratio on maximum efficiency.

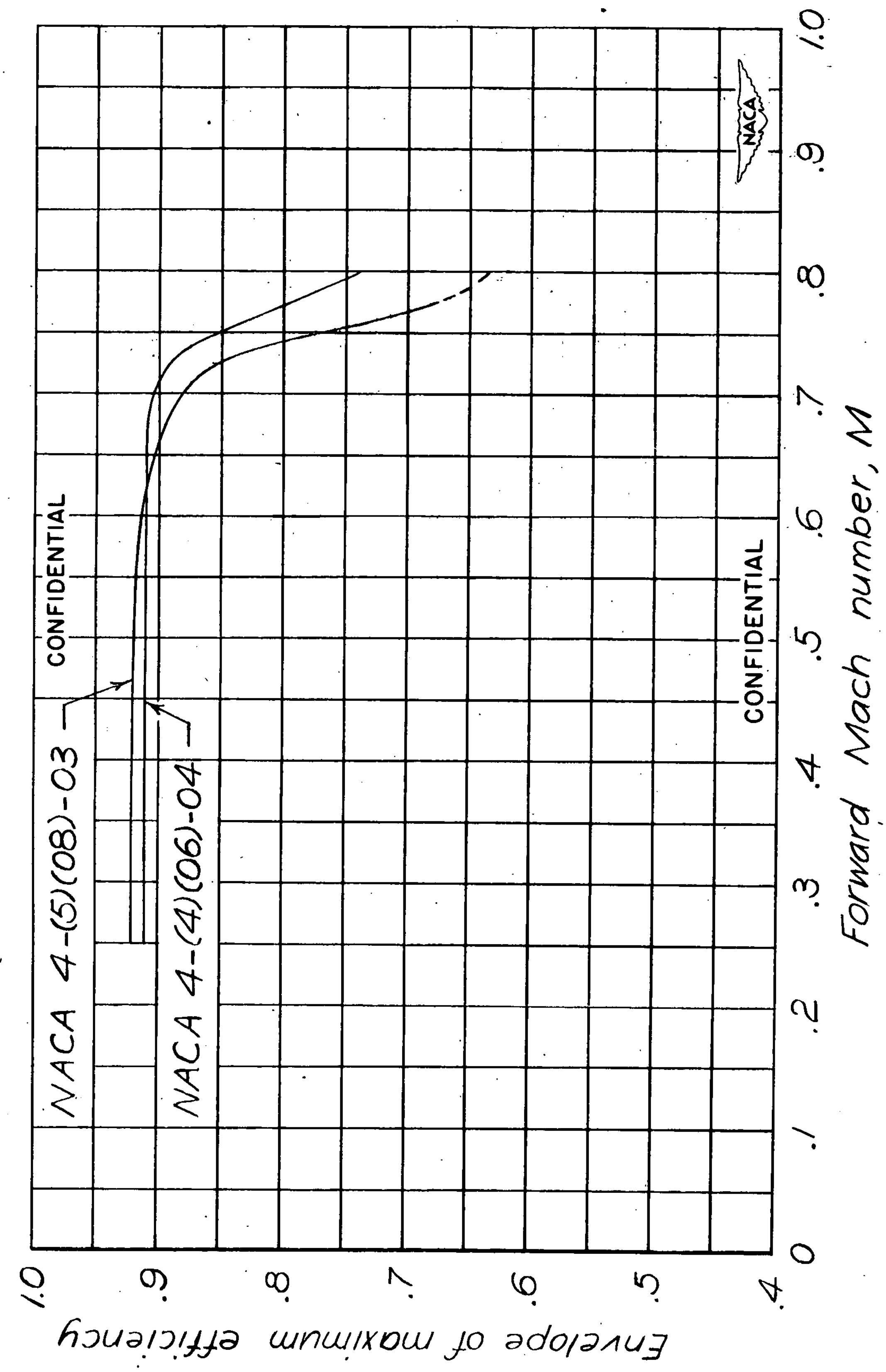

Figure 8.- Effect of forward Mach number on envelope efficiency.